International Journal of Bifurcation and Chaos

BOOLEAN DELAY EQUATIONS ON NETWORKS IN ECONOMICS AND THE GEOSCIENCES

BARBARA COLUZZI[a], MICHAEL GHIL[a,b,c], STÉPHANE HALLEGATTE[d,e], and GÉRARD WEISBUCH[a,f]

a) *Environmental Research and Teaching Institute, Ecole Normale Supérieure*, 24, rue Lhomond, F-75231 Paris Cedex 05, France.
b) *Geosciences Departement and Laboratoire de Météorologie Dynamique (CNRS and IPSL), École Normale Supérieure*, 24, rue Lhomond, F-75231 Paris Cedex 05, France.
c) *Department of Atmospheric & Oceanic Sciences and Institute of Geophysics & Planetary Physics, University of California*, Los Angeles, CA 90095-1565, USA.
d) *Centre International de Recherche sur l'Environnement et le Développement*, 4bis avenue de la Belle-Gabrielle, 94736 Nogent-sur-Marne Cedex, France.
e) *École Nationale de la Météorologie*, Météo-France, France.
f) *Laboratoire de Physique Statistique*, École Normale Supérieure, 24, rue Lhomond, F-75231 Paris Cedex 05, France.

We study damage propagation in networks, with an emphasis on production-chain models. The models are formulated as systems of Boolean delay equations. This formalism helps take into account the complexity of the interactions between firms; it turns out to be well adapted to investigating propagation of an initial damage due to a climatic or other natural disaster.
We consider in detail the effects of distinct delays and of forcing, which represents external intervention to prevent economic collapse. We also account for the possible presence of randomness in the links and in the delays. The paper concentrates on two different network structures, periodic and random, respectively; their study allows one to understand the effects of multiple, concurrent production paths, and the role played by the network topology in damage propagation. Applications to the recent network modeling of climate variability are discussed.

Keywords: damage propagation, directed graph, random graph, natural disasters, production chains

PACS: 02.30.Ks Delay and functional equations
89.65.Gh Economics; econophysics, financial markets, business and managements
89.75.Hc Networks and genealogical trees
91.30.Ab Theory and modeling, computational seismology
92.40.Cy Hydrology and glaciology: modeling; general theory
92.70.Aa Abrupt/rapid climate change

1. Introduction and motivation

1.1. *Motivation*

This paper is dedicated to the contributions of Catherine Rouvas-Nicolis to applying the concepts and tools of complex systems to a better understanding of weather and climate dynamics. There are two key connections between the paper and her contributions. First, much of the recent concerns with weather and climate have to do with possibly deleterious effects that global warming and its associated changes in the distribution of extreme events may have on the economy [Solomon et al., 2007; Ghil et al.*, 2011]. It is such deleterious effects that we study here, through a Boolean delay equation (BDE) model acting on several types of production-chain networks.*

Second, one of us (M.G.) developed BDEs as the result of reading Katy Nicolis's paper [Nicolis, 1982] that applied a related methodology, namely René Thomas's kinetic logic [Thomas, 1979], to an oscillatory paleoclimate model [Källén et al.*, 1979; Ghil, 1994]. Finally, there is a third, more general connection to climate dynamics, since network models of climatic teleconnections are gaining in popularity [Tsonis & Swanson, 2008; Donges* et al.*, 2009].*

1.2. *Background*

In most economic models, the production system is modeled either as a unique representative producer — e.g., by using the Cobb-Douglas function [Cobb & Douglas, 1928], as done in the Solow growth model [Solow, 1956] — or as a set of sectors, in which there is a unique representative producer per sector, e.g., in General Equilibrium Models [Arrow & Debreu, 1954]. The real production system, however, can best be seen as a network composed of firms that produce different goods and services, and are connected by links between suppliers and customers. In such a network, firm j supplies a fraction of its production to firm i, which uses this production as an input for its own production function; see [Fig. 1], for instance, in Section 2.1 below.

Introducing the role of networks in the economic system can lead to complex endogenous economic dynamics [Helbing *et al.*, 2004]. But the network formalism is also well adapted to study the cascade effects generated by exogenous events; these events are positive in the case of new orders from the market [Romanoff & Levine, 1981, 1986, 1981; Leung *et al.*, 2007; Bak *et al.*, 1993; Okuyama *et al.*, 2004; Barker & Santos, 2009] and negative in the case of a financial crisis [Delli Gatti *et al.*, 2005], of local strikes affecting production [Souma *et al.*, 2001; Weisbuch & Battiston, 2007] or of natural disasters [Hallegatte, 2008; Henriet, 2007; Henriet & Hallegatte, 2008; Henriet *et al.*, 2010]. In classical economic models — where the production system is modeled as a unique representative producer or as a small set of representative producers — the effects of exogenous events on the numerous firms have to be averaged over all firms, or over all firms of each sector. Because such effects are often highly heterogeneous, and because consequences and responses are highly nonlinear, this averaging process can bias the analysis, and hamper the correct assessment of the consequences of exogenous shocks, whether natural or man-made.

The case of natural disasters is particularly interesting, because disaster impacts are very heterogeneous and affect especially strongly a small set of firms [Tierney *et al.*, 1997; Webb *et al.*, 2002]. In such cases, the total economic impact of the catastrophe can be much higher than the direct impacts of the event, because indirect effects that are propagated through supply chains can be large. For instance, an earthquake that destroys a bridge can cause losses that are much larger than the value of the bridge, because subsequent impacts on the duration and cost of transportation can impair production in many firms.

Such results have been reported using input-output models [Leontief, 1986] at the sector level [Hallegatte, 2008; Henriet *et al.*, 2010; Lian *et al.*, 2007; Okuyama, 2004; Rose & Liao, 2005] or specific network models [Cho *et al.*, 2001]. To account for heterogeneity at the firm level, an appropriate input-output formalism has been developed in [Hallegatte, 2008; Henriet, 2007; Henriet *et al.*, 2010], and used to analyze disaster consequences. This approach has demonstrated that the shape and the structure of the network play an important role in disaster vulnerability, justifying the introduction of network effects in the economic assessment of natural disasters.

The purpose of the present paper is to simplify as much as possible the network formalism, by using

the flexible framework of Boolean delay equations (BDEs). The resulting models allow one to go beyond the simple observation that network structure has an influence on the problem, and permit one to analyze its effect on disaster consequences within an idealized economy. We study systematically and in detail the models, by emphasizing the differences in the dynamical behavior between forced vs. free models — *i.e.,* between externally connected vs. stand-alone models — and between asynchronous vs. synchronous updating for economic, production-chain networks. Possible applications to climatic networks are also discussed.

The simplification due to using Boolean variables allows one to study the effects of network topology and of the different delays involved in the production paths on the total losses due to an initial catastrophe. We investigate, in particular, the role of the network's connectivity: the effect of the multiplicity of products needed by each industry on the vulnerability of the whole economy, and the effects of multiple production paths from one firm to downstream production firms. We are especially interested by the spatio-temporal patterns of long-term production shortages that arise from the generic asynchrony due to variable time lengths of concurrent production paths.

In fact, the approach is intriguing from the more general point of view of local damage reverberation across a network, which is found in numerous and diverse fields of application. In the socio-economic domain, these fields include logistics [Bak *et al.*, 1993], infrastructures [Haimes & Jiang, 2001], and finance [Delli Gatti *et al.*, 2005; Battiston *et al.*, 2007], while in the geosciences they include earthquake dynamics [Zaliapin *et al.*, 2003a,b; Ghil *et al.*, 2008], forest fires [Spyratos *et al.*, 2007] and river networks [Zaliapin *et al.*, 2010], as well as climatic variability [Tsonis & Swanson, 2008; Donges *et al.*, 2009]. Finally, life-science applications include food webs [Carpenter *et al.*, 1985] and immunology [Kaufman *et al.*, 1985; Neumann & Weisbuch, 1992; Perelson & Weisbuch, 1997], among many others. Previous work on such problems has been restricted, however, to fairly simple network structures — such as ternary trees [Zaliapin *et al.*, 2003a,b; Ghil *et al.*, 2008], lattices [Bak *et al.*, 1993; Weisbuch & Battiston, 2007; Spyratos *et al.*, 2007], cartwheels [Delli Gatti *et al.*, 2005; Battiston *et al.*, 2007] or data-based scale-free networks [Henriet *et al.*, 2010] — and to purely autonomous dynamics; simple random forcing has only been considered in [Zaliapin *et al.*, 2003a,b] so far.

1.3. *This paper*

BDEs are semi-discrete dynamical systems, whose discrete variables evolve in continuous time; they have been introduced about 25 years ago by M. Ghil and colleagues [Dee & Ghil, 1984; Mullhaupt, 1984; Ghil & Mullhaupt, 1985], and they are related to the kinetic logic of R. Thomas [Thomas, 1979]. Unlike in the latter, though, the memory of a BDE system can contain more and more information as time goes on; this fact allows for solutions of increasing complexity, which display deterministically chaotic behavior. This prediction of BDE theory has been recently demonstrated experimentally in [Zhang *et al.*, 2009].

Apart from their intriguing mathematical properties, BDEs represent a useful tool in modeling complex systems that are characterized by threshold behavior, multiple feedbacks, and distinct time delays. They have been successfully applied, for instance, to the study of climate dynamics [Ghil *et al.*, 1987; Wright *et al.*, 1990; Darby & Mysak, 1993; Saunders & Ghil, 2001], of earthquake physics [Zaliapin *et al.*, 2003a,b], and of genetics [Öktem *et al.*, 2003; Gagneur & Casari, 2005]; see [Ghil *et al.*, 2008] for a recent review. The present work is an important step towards the application of BDEs to large classes of systems of interest in economics and in the geosciences; at the same time, it provides insight into the role played by stochasticity in Boolean-valued network models.

Even though we are using Boolean variables to describe the production of each individual firm, a zero value should not be interpreted as the destruction of the production unit: we simply mean that some shortage has been generated through production interactions. Similarly, a level of one only implies that the firm has recovered from a previous state of impaired production. Nevertheless, in the more general setting of local damage reverberation across a network, x_i can represent any form of healthy or damaged site.

In Section 2, we outline the Boolean-valued network models of the economy that we use throughout; they include *free* models, *i.e.* autonomous models of a closed economy, as well as *forced* models, *i.e.* non-autonomous models of an open economy. We moreover introduce the main observables we are interested

in: the density $\rho(t)$ of "healthy" firms, and the total number $\theta(t)$ of "damaged" ones; this intensive and extensive quantity, respectively, allow one to characterize the damage propagation. In Section 3, we present the results for free and forced models of degree one and higher on a periodic network, also referred to as having a chain topology; see [Fig. 1] below. One distinguishes already in this simple setting between the case of *synchronous* updating — *i.e.,* of deterministically chosen, equal delays — and the *asynchronous* case, *i.e.,* of randomly chosen delays that are unequal in general. Then, in Section 4, we consider directed random graphs, thus allowing for randomness in the links, *i.e.,* in the topology, as well as in the delays. Concluding remarks follow in Section 5, and three appendices provide technical details.

2. The models and their evaluation

2.1. *Model formulation*

A realistic representation of the economy at the firm level has to assess both the direct and the indirect losses due to either a natural or a man-made disaster. Doing so requires taking into account, in particular, the propagation of a disaster's consequences — both backward and forward in time — by tracking the avalanches of failures and the ripple effects across the chains of suppliers and producers in the network. For instance, analyses of the Northridge earthquake's impacts on the regional economy [Tierney *et al.*, 1997; Gordon *et al.*, 1998] show that a catastrophe can have very heterogeneous repercussions, and that indirect losses — due largely to damages to the transport infrastructure system — can be definitely higher than the direct losses themselves. Similar conclusions were obtained by the study of the consequences of the Loma Prieta and Northridge earthquakes [Webb *et al.*, 2002]. The latter study also showed that the repercussions can be less severe for firms that belong to a larger market, and not just to the strictly local one: this conclusion encourages us to consider economic models that adapt to a catastrophe by interacting with firms outside the immediately affected region, cf. [Cho *et al.*, 2001].

Important steps towards formulating input-output models [Leontief, 1986] suitable for realistic damage evaluations have been taken by S. Hallegatte and colleagues [Hallegatte, 2008; Henriet, 2007; Henriet & Hallegatte, 2008; Henriet *et al.*, 2010]. As stated in Section 1, we study here BDE models that are highly simplified in the sense that they only use Boolean-valued variables; on the other hand, they contain the dynamics of damage propagation, while allowing for unequal path lengths between firms in this propagation. We are neglecting some key ingredients, such as the division of the economy into sectors or the choice that firms might have between several providers of the same good, even in a strictly local economy. Therefore, the models highly idealized assumptions do not permit a direct application of their numerical results. These results, though, can be understood in depth, based on the complementary theories of graphs and of BDEs, and provide, one hopes, a good starting point for future analysis of more realistic damage propagation models.

A Boolean variable's null value, $x_i(t) = 0$, is taken to mean that firm i at time t is impaired and cannot fully produce, *i.e.* it is "damaged," while $x_i(t) = 1$ means that it is not impaired, *i.e.* it is "healthy." More specifically, the impairment can be due either to the firm being itself damaged or to the fact that it lacks the necessary inputs, since some of its suppliers — or some of their suppliers, and so on — were previously damaged. In this simple way, our BDE models take into account the role of the chains of suppliers and producers in a real economy.

We study networks of N firms, assumed to be placed at the vertices of a directed graph, also called a *digraph*; the digraph will be defined by its $N \times N$ *connectivity matrix* A, cf. [Bollobás, 1998; Bang-Jensen & Gutin, 2009]. Our interpretation is that $A_{ij} = 1$ if and only if (iff) part of the output of firm j (the supplier) is needed as input for firm i (the customer); otherwise $A_{ij} = 0$. As a first step for assessing the losses due to the propagation of the consequences of a catastrophic event, we analyze the vulnerability of connected firms to initial damage to a single firm. Considering the case of a single initial impairment is equivalent to studying the "Green's function" of damage propagation [Ghil *et al.*, 2008].

We start in Section 3 by considering a connectivity matrix A with circulant structure, which models a *braid chain* of in/out-degree k: $A_{ij} = 1$ iff $i - k \leq j \leq i - 1$, with $x_i = x_{i+N}$ (see [Fig. 1]). In Section 4, we will study a directed random graph (DRG) or random digraph. We will concentrate on the DRG family $D(N, p)$ [Karp, 1990; Łuczac & Seierstad, 2009], obtained by generalizing the well-known Erdős-Rényi rule

for an undirected random graph [Erdős & Rényi, 1959, 1960, 1961]; in our DRG, each of the $N(N-1)$ directed links is present or absent with the same independent probability $p \in [0,1]$. Hence, the elements $\{A_{ij}\}$ of the matrix A are random variables, assumed to be independently and identically distributed, with probability $\mathcal{P}$ given by

$$\mathcal{P}(A_{ij}) = \begin{cases} \delta_{A_{ij},0}, & i = j; \\ p\,\delta_{A_{ij},1} + (1-p)\,\delta_{A_{ij},0}, & i \neq j; \end{cases} \tag{1}$$

where δ is the Kronecker delta function. The probability p is related in a straightforward manner to the mean number of input-output connections z, *i.e.* to the average in/out-degree $\langle k \rangle$ of the resulting digraph, with $z = \langle k \rangle = (N-1)p \simeq Np$.

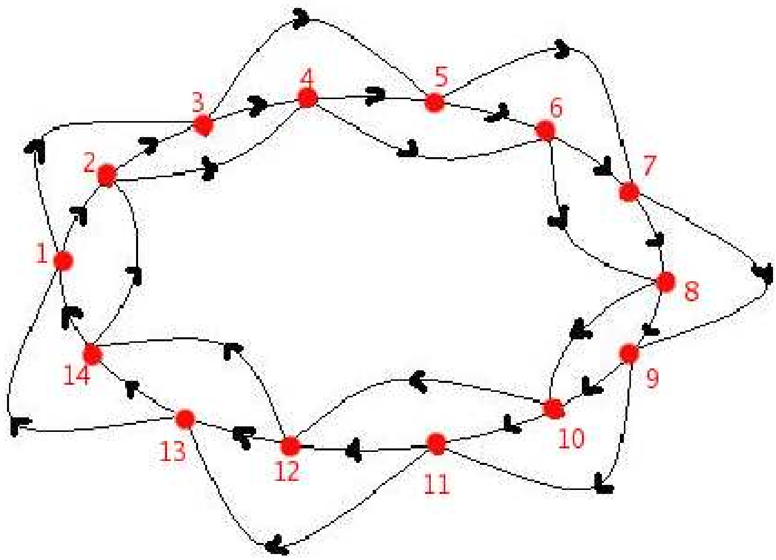

Fig. 1. The braid-chain structure given by a circulant matrix with periodic boundary conditions, in the case of an in/out-degree $k = 2$. The size of the network here is $N = 14$, and the nodes are ordered clockwise. In the synchronous deterministic model with equal delays, the position of the origin — always chosen to be $i = 1$ — is arbitrary. In the asynchronous case of random delays, the distinct concurrent paths that connect two given nodes do not involve, in general, the same propagation time, although they might have the same spatial length, in terms of number of steps along the chain. Unless confusion is possible, we refer to "path length" as the *time* it takes to get from a node to another.

The dynamics on the network defined by the matrix $A = \{A_{ij}\}$ is governed by the system of N BDEs:

$$x_i(t) = \prod_{j=1}^{N} \overline{A}_{ij} \vee S_{ji}(t), \qquad i = 1, \ldots, N; \tag{2}$$

here $S_{ji}(t)$ is the availability of good j at node i. The product $\prod$, which runs over all the vertices of the network, refers to the Boolean 'AND' operator $\wedge$, whereas $\vee$ denotes the Boolean 'OR' operator and $\overline{(\cdot)}$ is the Boolean negation.

Notice that, in our highly idealized models, the production $x_i(t)$ of firm i at time t requires the availability of all the stocks of goods $S_{ji}(t)$ usually provided by the suppliers $\{j : A_{ij} \neq 0\}$ to which the firm i is connected in the network. In other words, a firm's production capacity can be impaired either by a disaster having directly damaged it or because its suppliers have been affected by the disaster and cannot provide the necessary inputs. We will assume that only a single firm is directly damaged at the beginning,

Table 1. The input-output table of the stock S_{ji} of a given product as a Boolean function of the activities (x_i, x_j) of the customer firm i and supplier firm j, in the free models described by Eq. (3) and in the forced models described by Eq. (4), respectively.

x_i	x_j	S_{ji}	Free models
0	0	0	j and i inactive, the stock cannot be reconstituted
0	1	1	j active and i inactive, the good is stocked
1	0	0	j inactive and i active, the stock is finished
1	1	1	j active and i active, the stock is updated
x_i	x_j	S_{ji}	Forced models
0	0	1	j and i inactive, the stock is supplied from outside
0	1	1	j active and i inactive, the good is stocked
1	0	0	j inactive and i active, the stock is finished
1	1	1	j active and i active, the stock is updated

so that its production is reduced during a time interval of length τ_c, and we will look at the propagation of this initial event.

We consider first isolated networks, which we call the *free* models, and then networks that interact with the outside, the *forced* models; the forcing represents external intervention to prevent economic collapse. For a free model, the availability S_{ji} of the good manufactured by firm j to firm i is simply delayed with respect to the production x_j by a constant *delay* τ_{ij} according to:

$$S_{ji}(t) = x_j(t - \tau_{ij}), \qquad \text{for a free model.} \tag{3}$$

In the presence of socio-economic adaptability — meaning that the local economy of the immediately affected region is not isolated, and that some external rescue input is available — we assume that the production stock S_{ji} of the firm i becomes again available to firm j after an impairment time taken, in a first approximation, to be still equal to τ_{ij}:

$$S_{ji}(t) = \overline{x}_i(t - \tau_{ij}) \vee x_j(t - \tau_{ij}), \qquad \text{for a forced model.} \tag{4}$$

These two equations, which give the truth table shown in [Tab. 1], complete the definitions of the models given by Eq. (2).

We compare in the following results obtained for equal delays $\{\tau_{ij} \equiv \tau_0\}$ with those for the more realistic situation of a set $\mathcal{T}$ of unequal delays $\{\tau_{ij}\}$ picked at random. We refer to these two situations as *synchronous* and *asynchronous* updating, respectively. Notice that the latter term is given here a different meaning from the one usually found in the literature on random Boolean networks [Drossel, 2008]. In our asynchronous BDE models, the delays are assumed to be integer multiples of the time unit given by $\tau_{\min}$, and to be independently and uniformly distributed in the interval $[\tau_{\min}, \tau_{\max}]$, where $\tau_{\max}$ is also an integer multiple of $\tau_{\min}$.

In the numerical computations, we will take $\tau_0 = \tau_{\min} = 1$ day and $\tau_{\max} = 10$ days. Notice that, for a given set $\mathcal{T}$ of randomly selected delays and for a randomly selected set of links — which we will also call a random network configuration Ω — the smallest nearest-neighbor delay,

$$\tau^*(\Omega, \mathcal{T}) = \min_{i,j}\{\tau_{ij}\}, \tag{5}$$

can be larger than $\tau_{\min}$, although the probability of this event approaches rapidly zero as the network's size N increases. We summarize in [Tab. 2] the various BDE-on-network models studied in this paper, and provide in [Tab. 3] a list of the main variables and other symbols used herein.

In order to get a unique solution of either a free model, given by Eqs. [(1), (2), (3)] or of a forced model, given by Eqs. [(1), (2), (4)], one has to prescribe the initial values of the set of variables $\{x_i(t)\}$ in the interval $[0, \tau_{\text{init}})$, where $\tau_{\text{init}} = \max\{\tau_{ij}\}$ is the largest possible delay, with $\tau_{\text{init}} = \tau_0$ for synchronous and $\tau_{\text{init}} = \tau_{\max}$ for asynchronous updating. We only study here the simple case in which the entire economy $\{i : 1 \le i \le N\}$ starts unimpaired, except for the initial destruction of a single firm, which is taken without

Table 2. Overview of the main characteristics of the models studied in Sections 3 and 4; each box in the table indicates the section where the model defined by the row and column is discussed. In the columns, we label by **Free** the free models and by **Forced** the forced models; the synchronous case of deterministic delays all equal to τ_0 is labeled **Sync** and the asynchronous, random-delay case is labeled **Async**. In the rows, **Chain** refers to the deterministic braid chain of [Fig. 1], and **DRG** to the random digraph, with $\mathcal{P}(A_{ij})$ given by Eq. (1). In the rows, we also distinguish between single ($k = 1$), and multiple ($k \geq 2$), in/out-degree in the braid chain, whereas the models defined on the digraph whose average in/out-degree $z = \langle k \rangle$ is either equal to or larger than one are treated in the same sections.

	Free, Sync	Free, Async	Forced, Sync	Forced, Async
Chain, $k = 1$	3.2	3.3	3.6	3.6
Chain, $k \geq 2$	3.4	3.5	3.7	3.8
DRG	4.2	4.3	4.4	4.4

loss of generality to be at the node $i = 1$. Notice that this firm is not definitively eliminated form the network: we assume instead that it is forced to stop its activity from time $t = 0$ until $t = \tau_c$. Hence we will usually take $x_i(t) \equiv 1$ for $t \in [0, t_{\text{init}})$, except for $x_1(t) = 0$ for $t \in [0, \tau_c)$, with $\tau_c \leq t_{\text{init}}$. More generally, one can associate an external function to the x_1-variable, *i.e.* $x_1(t) \to \mu(t)x_1(t)$, where $\mu(t)$ is taken to be one except for $t \in [0, \tau_c)$: this allows one to appropriately describe also the case $\tau_c > \tau_{\text{init}}$.

The possibility of defining BDE systems that possess random delays with a given probability distribution was already stated in [Dee & Ghil, 1984], but BDE studies so far have been mainly restricted to fully deterministic systems. Two exceptions are the results in [Wright *et al.*, 1990], where the ensemble averaging over BDE solutions with randomized initial data was considered, and in [Zaliapin *et al.*, 2003a,b], where random external forcing was introduced. We study here in considerable detail not only BDEs with random delays, but also BDEs on a random graph (cf. Section 4 below), as suggested in [Ghil *et al.*, 2008]; the latter could also be viewed as Boolean networks with distinct delays [Öktem *et al.*, 2003; Klemm & Bornholdt, 2005].

In the present paper, the exploration of *stochastic* BDEs is limited to the delays $\mathcal{T} = \{\tau_{ij}\}$, as well as the elements of the connectivity matrix $\{A_{ij}\}$, being *quenched* random variables: their values are prescribed once and for all when defining the BDE system. The random configuration $\{\Omega, \mathcal{T}\}$ so obtained is assumed here to be constant on the time scale of the system evolution we are interested in. Random evolution in time of the set of links Ω, as well as of the set of delays $\mathcal{T}$, is left for subsequent study. We note here simply that — in statistical physics in general and in spin-glass theory in particular — a system is said to present *quenched disorder* when some parameters that determine its behavior are random variables that do not evolve with time, *i.e.*,they are quenched or frozen [Mézard *et al.*, 1988].

2.2. *Evaluation of model behavior*

To facilitate the comparison between the results of these models, and to help us draw general conclusions about damage propagation in economic networks, we introduce here two global quantities that characterize model behavior. The first one of these two macroeconomic observables is the density $\rho(t)$ of "healthy" firms, which is given simply by the average over the number N of nodes:

$$\rho(t) \equiv \frac{1}{N} \sum_{i=1}^{N} x_i(t). \tag{6}$$

As noted before [Ghil *et al.*, 2008], the evolution of a single impairment represents the "Green's function" of damage propagation, and $\rho(t)$ is just a key property of this Green's function.

For obvious reasons, we will be especially interested in the large-time limit, so that we also find it useful to define the *asymptotic* density:

$$\rho_\infty = \lim_{t \to \infty} \rho(t). \tag{7}$$

Table 3. Overview of the main variables and symbols that appear in the paper.

$x_i(t)$	Boolean variable: state of firm i (more generally, node i) at time t
N	integer variable: total number of firms, *i.e.* system size
S_{ij}	Boolean variable: stock provided by supplier j to customer i
$A = \{A_{ij}\}$	$N \times N$ connectivity matrix A, whose elements are the Boolean variables A_{ij}
$\Omega = \{A_{ij}\}$	random network configuration, *i.e.*, set of random links
$\mathcal{T} = \{\tau_{ij}\}$	the $N \times N$ set of delays τ_{ij}
$D(N,p)$	DRG family of size $N \times N$, whose links are present with probability p
$G(N,p)$	undirected random graph of size $N \times N$; links have probability p
k, $k_{\rm in}$, $k_{\rm out}$	degree, in-degree, out-degree
$z = \langle k \rangle$	mean connectivity in random networks
$\tau_{\rm c}$	duration of the initial event
τ_0	delay and time unit in the synchronous models
$\tau_{\rm min}$	smallest delay and time unit in the asynchronous models
$\tau_{\rm max}$	largest delay in the asynchronous models
$\tau_{\rm init}$	largest possible delay, depending on the model
$\tau^*(\Omega, \mathcal{T})$	smallest nearest-neighbor delay
$\mu(t)$	external function
ϖ	period of the asymptotic solution
θ	total number of impaired firms
ρ	density of fully active firms
ρ_∞	asymptotic time limit of the density
ρ_∞^ϖ	asymptotic time limit of the density averaged over the period
T_0	effective transient: time for ρ to reach ρ_∞
T_ϖ	transient: time that system solutions take to reach the asymptotic regime, $T_0 < T_\varpi$
v	signal velocity
$\mathcal{C}_{ij}$	path joining nodes i and j
$\mathcal{S}_c$	connected component of size $S_c = s_c N$
$\mathcal{S}_{gc}$	giant connected component of size $S_{gc} = s_{gc} N$
r	fraction of nodes outside the giant connected component
$\mathcal{S}_{sc}$	giant strongly connected component of size $S_{sc} = s_{sc} N$
$\mathcal{I}$	giant in-component of size $I = s_I N$
$\mathcal{O}$	giant out-component of size $O = s_O N$
$\mathcal{W}$	giant weakly connected component of size $W = s_w N$
Θ	other giant component defined as $\Theta = \mathcal{W} \setminus (\mathcal{I} \cup \mathcal{O})$
$z_{\rm c}$	critical value of the mean connectivity
δ	Kronecker delta function
$\overline{(\cdot)}$	Boolean negation (unary operator)
$\vee$	Boolean AND (binary operator)
$\wedge$	Boolean OR (binary operator)
$\veebar$	Boolean XOR (binary operator)
$\langle\langle(\cdot)\rangle\rangle$	average over the quenched random configurations

In the presence of asymptotically periodic solutions, one obviously considers the period average:

$$\rho_\infty^\varpi = \lim_{t\to\infty} \int_t^{t+\varpi} \rho(t')\mathrm{d}t'. \tag{8}$$

The quantities ρ_∞ or ρ_∞^ϖ represent the fraction of the economy that finally recovers from the initial damage, *i.e.* a value of ρ_∞ equal to one means that the economy will recover completely, whereas on the contrary $\rho_\infty = 0$ implies that lasting damage propagates across the entire network. Within our framework, it will be possible, in particular, to understand the behavior of the asymptotic density in the case of large N and of $N \to \infty$.

The second macroeconomic observable of interest is the total number $\theta(t)$ of impaired firms at time t. In the thermodynamic language of statistical physics, $\theta(t)$ is an extensive variable, while $\rho_\infty(t)$ is intensive. The observable $\theta(t)$ gives directly the total losses, at a given time, due to the initial destruction of the

single firm at $i = 1$; hence $\theta(t)$ is also a measure of damage spreading, due to its propagation through the network. We have

$$\theta(t) \equiv \sum_{i=1}^{N} \overline{x}_i(t). \tag{9}$$

Notice that the average density $\rho(t)$ of "healthy" firms and the total number $\theta(t)$ of impaired firms are related by

$$\rho(t) = 1 - \frac{1}{N}\theta(t). \tag{10}$$

We will also study three highly nonlinear functionals with the physical dimensions of time: the effective transient T_0, defined as the time that the density takes before reaching its asymptotic ρ_∞ value; the transient T_ϖ, defined as the time elapsed before the solutions become periodic; and the period ϖ of the solution itself, possibly equal to zero if the solution is constant. Notice that, since the delays here are rationally related, the asymptotic solutions of the BDE system (2) are necessarily constant or periodic, because of general results on BDEs [Ghil *et al.*, 2008; Dee & Ghil, 1984; Mullhaupt, 1984; Ghil & Mullhaupt, 1985]. Nevertheless, we will find very long transients and periods and, moreover, one can have $T_\varpi \gg T_0$.

In the presence of randomness — in the delays, in the elements of the connectivity matrix or in both — these quantities do also depend upon the particular configuration $\{\Omega, \mathcal{T}\}$, and the system's behavior is better captured by their *average* value. In the case of the density, one has:

$$\langle \rho(t; \Omega, \mathcal{T}) \rangle \equiv \int \mathrm{d}\mathcal{T}\mathrm{d}\Omega \mathcal{P}(\Omega, \mathcal{T}) \rho(t; \Omega, \mathcal{T}). \tag{11}$$

This average can be computed numerically by considering a large enough number $\mathcal{N}_s$ of random configurations $\{\Omega, \mathcal{T}\}$: in fact, these are obtained in agreement with their corresponding $\mathcal{P}(\Omega, \mathcal{T}) = \mathcal{P}(\Omega)\mathcal{P}(\mathcal{T})$, *i.e.* with uniform probability in the interval $[\tau_{\min}, \tau_{\max}]$ for the random-delay case of asynchronous updating, and with probability given by Eq. (1) for the random links of the DRG. Generally, we will spell out the dependence of an observable O upon the configuration, by labeling it $O(\Omega)$, $O(\mathcal{T})$ or $O(\Omega, \mathcal{T})$, accordingly, and we will label its average value, computed analogously to the average density in Eq. (11), by $\langle O(\Omega) \rangle$ and so on.

3. Braid-chain models

3.1. *Network topology*

We consider here the network topology of a braid chain, which is obtained from an $N \times N$ connectivity matrix A with circulant structure: $A_{ij} = 1$ iff $i - k \leq j \leq i - 1$, with $x_{i+N} = x_i$. Here one has the same in/out-degree k for all the nodes: each firm needs as inputs part of the goods manufactured by the previous k firms (its suppliers), whereas the outputs it produces are used by the k next firms (its customers); so each firm is linked to $2k$ other firms.

The resulting deterministic topology is *strongly connected*: starting from any node one finds at least one directed path along which the signal can propagate to any other node, and in fact there are multiple concurrent paths as soon as $k \geq 2$. Most of these paths have the same length in the purely deterministic case of synchronous updating, whereas their lengths usually differ for asynchronous updating. In other words, randomly chosen delays allow one to model the distinct times that damage propagation along the concurrent production paths may take. The example in [Fig. 1] has an in/out-degree of $k = 2$.

When A is a circulant matrix, the equations for each x_i in system (2) simplify to yield:

$$x_i(t) = \prod_{j=1}^{k} x_{i-j}(t - \tau_{i,i-j}), \tag{12}$$

for the free model defined by Eq. (3), and

$$x_i(t) = \prod_{j=1}^{k} \overline{x}_i(t - \tau_{i,i-j}) \vee x_{i-j}(t - \tau_{i,i-j}), \tag{13}$$

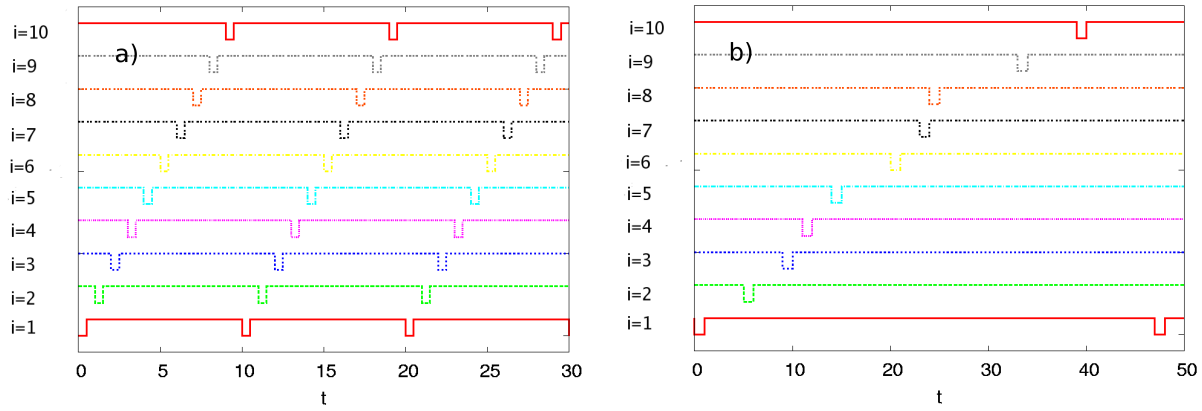

Fig. 2. Time evolution of the state of the 10 nodes of the free model on a braid chain, with $k = 1$, after an initial perturbation of node $i = 1$. Each Boolean variable $x_i(t)$ is plotted as a function of t: it is a piecewise constant function alternating between 0 and 1. The plot for each node i is shifted along the y axis, to help visualize the wave that propagates across the network. (a) All the delays are equal to $\tau_0 = 1$ day, the duration of the initial perturbation is $\tau_c = \tau_0/2 = 0.5$ day, and the period of the wave is $\varpi = N\tau_0 = 10$ days. (b) A particular evolution for a given choice $\mathcal{T}$ of random delays, with $\{\tau_{i,i-1}\}$ uniformly distributed between $\tau_{\min}$= 1 day and $\tau_{\max}$=10 days: the resulting period is $\varpi(\mathcal{T}) = 47$ days; here the duration of the initial perturbation is $\tau_c = \tau_{\min}/2$.

for the forced model defined by Eq. (4), respectively. The study of BDEs for this highly simplified topology has two advantages: (i) it allows one to compare numerical with analytical results; and (ii) it facilitates a first glimpse at the substantial differences between free and forced models, on the one hand, and between synchronous and asynchronous forcing, on the other.

3.2. *Synchronous free model with* $k = 1$

The free model on a braid chain, with a single input-output connection for each node, $k = 1$, and with delays that are all equal to the same time unit τ_0, is an example of a *conservative* system of BDEs [Ghil *et al.*, 2008; Mullhaupt, 1984; Ghil & Mullhaupt, 1985]. Its dynamics is periodic right away, without any transient, for all initial states. The model obeys the set of equations:

$$x_i(t) = x_{i-1}(t - \tau_0), \qquad i = 1, \ldots, N. \tag{14}$$

The initial impairment of the single firm at $i = 1$ is usually represented, for a duration of $\tau_c \leq \tau_0$, by the appropriate choice of the initial values: one takes $x_i \equiv 1$ for $t \in [0, \tau_0)$, except for $x_1(t) = 0$ in the interval $[0, \tau_c)$. As stated in Sec. 2.1, to describe both the case $\tau_c \leq \tau_0$ that we treat here most often, and the case of $\tau_c > \tau_0$, one can replace $x_1(t)$ by $\mu(t)x_1(t)$, and let $\mu_1(t) = 0$ for $t \in [0, \tau_c)$.

The spatio-temporal pattern of the solution displays a wave of nodes taking the value zero for a duration τ_c, one after the other; this wave propagates periodically across the chain, as in the example given in [Fig. 2a]. Moreover, $\forall \tau_c < \tau_0$, the evolution shows no transient and the period of the solution is $\varpi = N\tau_0$. For $\tau_c > \tau_0$, the starting perturbation cannot be absorbed into the initial values, and the transient length is $T_0 = T_\varpi \simeq \tau_c - \tau_0$. Finally, we notice that, for $\tau_c = \tau_0$, the density is constant, $\rho(t) = \rho_\infty = 1 - 1/N$, whereas for $\tau_c < \tau_0$ it is a piecewise constant function that alternates between the values 1 and $1 - 1/N$, with period $\varpi = \tau_0$.

In fact, this system is almost exactly the same as the model introduced in [Ghil *et al.*, 2008] as a first step towards formulating the BDE equivalent of hyperbolic partial differential equations. In that paper, the simplest wave equation was discretized on a one-dimensional lattice, and the node index i played the role of the discretized coordinate; see Eq. (32) in [Ghil *et al.*, 2008]. Results were given for the evolution starting from an initial state in which only the variable associated with a single lattice point — located at the origin of the spatial coordinate — was equal to one, with $\tau_c = \tau_0$, while all other nodes carried zero values. These results were precisely the complement of those shown in [Fig. 2a], with a "soliton" of unit values propagating along the lattice (not shown in [Ghil *et al.*, 2008]).

This dynamics implies that, on the one hand, the damage does not spread to a larger number of firms but, on the other hand, the activity never recovers completely: each impaired firm gets back to the unaffected state after the time τ_c but, at the same time, its production shortage reaches its unique customer, with a constant delay τ_0. This result may look unrealistic, and in fact it is linked to one of our simplifying assumptions, namely the discretization of firm production capacity, with no possibility for overproduction or production rescheduling. Nevertheless, notice that $\rho_\infty = 1 - 1/N$, which means that, for a unit initial damage, the whole economy turns out to be still quite "healthy", apart from corrections of order $1/N$, which are negligible in the large-size limit.

3.3. *Asynchronous free model with $k = 1$*

In the free model on a braid chain, with $k = 1$, the effect of random, but integer-valued delays can be worked out explicitly. One gets

$$x_i(t) = x_i\left(t - \sum_{j=0}^{N-1} \tau_{i-j,i-j-1}\right) \tag{15}$$

and finds, accordingly, that the solution is periodic right away for any duration of the initial perturbations $\tau_0 \leq \tau^*(\mathcal{T})$; here $\tau^*(\mathcal{T})$ equals the smallest nearest-neighbor propagation length, defined as in Eq. (5), and it is usually equal to $\tau_{\min}$.

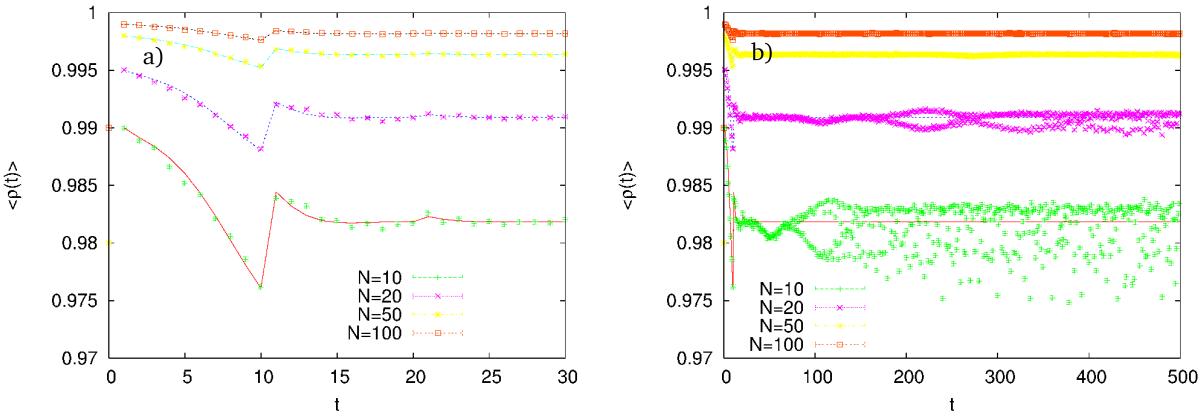

Fig. 3. Evolution of the average fraction $\langle \rho(t;\mathcal{T}) \rangle$ of fully active firms, in the asynchronous free model on a braid chain, with $k = 1$; here $\tau_c = \tau_{\min}$. We compare the behavior of networks having $N = 10$, 20, 50 and 100 nodes with the one expected from the CLT (lines); see Eq. (52) in Appendix A. (a) Detailed behavior at short times; (b) model behavior over the entire time window calculated. The data are averaged over $\mathcal{N}_s$ different random sets of delays $\mathcal{T}$, with $\mathcal{N}_s$ taken large enough to give errors of the order of the point size in the plot.

The spatio-temporal pattern of the solution is still a periodically propagating wave of nodes that take the value zero for a duration of τ_c, one after the other, cf. [Fig. 2b]; moreover, $\forall \tau_c \leq \tau^*(\mathcal{T})$, the evolution shows no transient, as in the synchronous case for $\tau_c \leq \tau_0$. The difference is that the propagation time of the perturbation, from a supplier $i-1$ to its customer i, is now given by the quenched random variable $\tau_{i,i-1}$. Hence the period $\varpi(\mathcal{T})$ of the solution, — depending upon the given random configuration of delays $\mathcal{T}$ — is equal to the sum of these delays along the whole chain, with an average value of $\langle \varpi(\mathcal{T}) \rangle = N(\tau_{\max}+1)/2$.

The average density $\langle \rho(t;\mathcal{T}) \rangle$ can be computed analytically by applying the central limit theorem (CLT), cf. Appendix A. In [Fig. 3], we compare the expected behavior for $\tau_c = \tau_{\min}$, given by Eq. (52) in the appendix, with the numerical results, for different network sizes N: at short times, one can observe the predicted jumps at $t = \tau_{\max}$. At long times, there are corrections to the expected behavior, since the same variables appear more than once in the sums of randomly selected delays that are being considered; nevertheless, the average asymptotic value of the density, $\langle \rho_\infty(\mathcal{T}) \rangle$, clearly approaches unity in the limit of

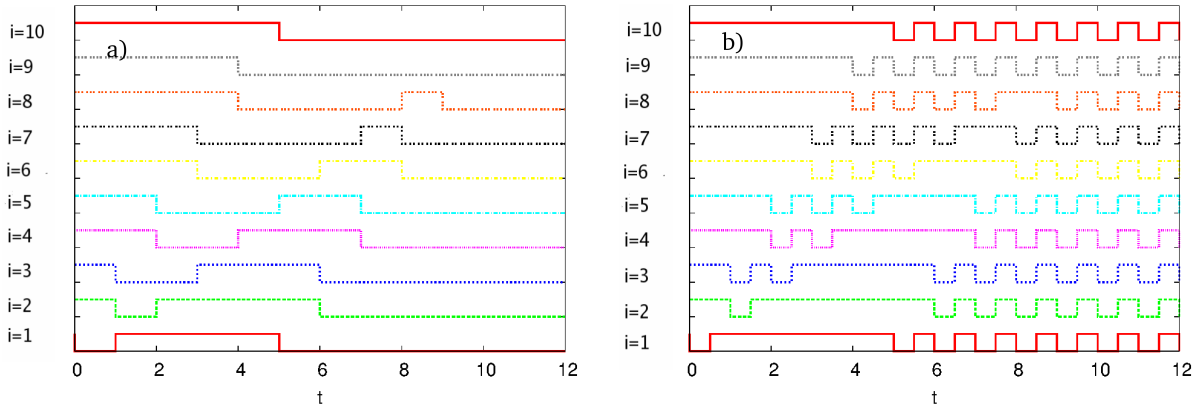

Fig. 4. Time evolution of the state of the 10 nodes of the synchronous free model on a braid chain, with $k = 2$, after an initial perturbation of node 1. Same plotting convention as in [Fig. 2]. (a) The duration of the initial perturbation is $\tau_c = \tau_0 = 1$ day; (b) $\tau_c = \tau_0/2 = 0.5$ day. See text for details.

large system size, with corrections of order $1/N$; more precisely, $\langle \rho_\infty(\mathcal{T}) \rangle \simeq 1 - 0.2/N$, in good agreement with Eq. (54) of Appendix A.

We stress therefore that in these free models on a braid chain with $k = 1$, the choice of updating, whether synchronous or asynchronous, is relatively unimportant, and a small initial damage has a negligible effect on the whole economy, when looking at a large number N of firms.

3.4. *Synchronous free model with $k \geq 2$*

As soon as the number k of connections is larger than one, the dynamics of the free model on the braid chain turns out to be *dissipative* [Mullhaupt, 1984; Ghil & Mullhaupt, 1985; Ghil *et al.*, 2008]. In simple terms, one expects OR operators to favor a steady state with $x_i \equiv 1$, while AND operators favor such a state with $x_i \equiv 0$. In fact, for synchronous models of cellular-automaton type, the propagation of 0 across networks that are characterized by the exclusive presence of AND operators is well documented [Weisbuch, 1991; Wolfram, 1994].

General results on BDEs [Mullhaupt, 1984; Ghil & Mullhaupt, 1985; Ghil *et al.*, 2008] establish that the asymptotically stable solution is the state in which the whole economy is attained by the consequences of the initial damage. Therefore the configuration $x_i \equiv 0$ is reached in finite time for any duration $\tau_c \geq \tau_0$ of the starting perturbation; see [Fig. 4a]. This result can be interpreted in terms of lack of flexibility in the system's behavior, since the k different inputs to a given firm are linked by AND operators alone. Besides, the system is isolated and the topology of the deterministic network is strongly connected.

To analyze the behavior in [Fig. 4a] more closely, let us start the discussion from the case $\tau_c = \tau_0$, where $\tau_0 = 1$ day, and assume that in the interval $[t, t+1)$ there are $\theta(t) = n$ impaired firms in consecutive positions along the chain, *i.e.*, $x_i(t) = 0$ for $i \in [i_{\rm hr}(t), i_{\rm min}(t)]$, with $i_{\rm hr}(t) = i_{\rm min}(t) + n - 1$ and $n \ll N$. Imagine now a clock that, at time t, has its hour-hand marking the position $i_{\rm hr}(t)$ of the impaired firm nearest to the origin, while the minute-hand marks the position $i_{\rm min}(t)$ of the one farthest from the origin. At each time step $t' = t + 1$, the firms in the next k positions (with $k \ll N$) after $i_{\rm min}(t)$ will be impaired, since at least one of the stocks that they need is not available; hence $i_{\rm min}(t') = i_{\rm min}(t) + k$.

The first firm in the sequence does recover its unaffected state, since all its suppliers are fully active; hence $i_{\rm hr}(t') = i_{\rm hr}(t) + 1$. In other words, both the hour-hand and the minute-hand move with constant velocities, given respectively by $v_{\rm h} = 1$ and $v_{\rm m} = k$; therefore the width of the set of "damaged" firms increases itself with constant velocity, and correspondingly one gets $\theta(t') = \theta(t) + (k - 1)$. Notice that this description is correct, in particular, when a single firm is damaged in the first time interval, as assumed herein.

The same argument can be applied again, at time $t = t'$, starting from the new sequence of states, and so on. It follows that the evolution will stop after the transient time $T_0 = T_\varpi$, when the minute-hand

catches up with the hour-hand, the former having gone around the chain one more time than the latter: the system has attained the asymptotically stable steady state $x_i \equiv 0$, and the economic activity can no longer recover at all. The result is unchanged if, in the last time step of the transient, the minute-hand passes the hour-hand, since $x_i = 0$ also describes a shortage in the production of firm i itself, aside from the lack of goods to be provided by other firms. Moreover, during the transient, each firm can recover at most once.

To summarize, $\theta(t)$ increases linearly with t until it reaches the system size N; correspondingly, for an initial perturbation that destroys the production of one firm for a duration $\tau_c = \tau_0 = 1$ day, $\rho(t) = 1 - 1/N - (k-1)t/N$ for $t \lesssim T_0$ and $\rho(t) = \rho_\infty = 0$ for $t > T_0$, where the length of the transient is given by:

$$T_0 \simeq \frac{N-1}{k-1}\tau_0. \tag{16}$$

These results are confirmed by the analysis given in Appendix B, where $\theta(t)$ is computed explicitly. Moreover, when considering $\tau_c > \tau_0$, for reasonable values of $\tau_c \ll k \ll N$, one has the same kind of behavior after roughly the first τ_c/τ_0 time steps: for large t, the damage-spreading velocity is constant and equal to $k-1$, and the length of the transient is still of order N/k.

For $\tau_c < \tau_0$, a typical solution is shown in [Fig. 4b]. Its spatio-temporal pattern clearly indicates that the damage spreads, from the initially damaged firm, across the whole network. Taking

$$x_1(t) = \begin{cases} 0 & \text{for} \quad t \in [0, \tau_c); \\ 1 & \text{for} \quad t \in [\tau_c, \tau_0 = 1), \end{cases} \tag{17}$$

the asymptotic steady state is periodic in space, with a period $T_\varpi = 1$, and all the firms are synchronously impaired only in the first τ_c part of each period; this periodic state is reached after a transient of length given again by Eq. (16). Notice that, in this case, the asymptotic density ρ_∞ is a piecewise constant function that alternates between the values zero and one with period $\tau_0 = 1$ day.

3.5. *Asynchronous free model with $k \geq 2$*

Notice first that, in this case, the damage cannot spread more slowly than in the particular case in which all the delays are equal to $\tau_{\max}$: it follows that the state $x_i \equiv 0$ is asymptotically stable also for asynchronous updating, and that it is reached no later than after a transient $T_0(\mathcal{T}) = T_\varpi(\mathcal{T})$. This is certainly the case as soon as $\tau_c \geq \tau_{\max}$; in fact we find that it is usually so as soon as $\tau_c \geq \tau_{\min}$.

Nevertheless, concurrent paths with the same space length along the chain do not usually have, in this case, the same time length, since different random variables appear now in the sums of the intervening delays. Hence the spatio-temporal pattern of the solution is more complex, as shown in [Fig. 5]. In particular, for $\tau_c < \tau_{\max}$, each firm can be impaired and recover more than once.

Since the delays are independently and identically distributed along the whole chain, one can argue that, in the limit $1 \ll t \ll T_0(\mathcal{T})$, the damage spreads with constant average velocity v: the lower bound on this quantity can be easily obtained, following the discussion in the previous Section 3.4, by taking all the delays equal to $\tau_{\max}$. The corresponding upper bound is obtained by setting all the delays equal to $\tau_{\min}$; hence $(k-1)/\tau_{\max} \leq v \leq k-1$. As we are going to show, because of the network structure and of the variables being linked by AND operators, of these two bounds, the upper bound is usually a definitely better approximation to the average velocity than the lower one, and one can obtain a much better lower bound, too.

To clarify this point, we use once again the clock-hand analogy, with the hour-hand marking the position $i_{\mathrm{hr}}(t)$ of the impaired firm nearest to the origin and the minute-hand the position $i_{\min}(t)$ of the impaired firm farthest from it: the key ingredients are that the network is a braid chain and that a firm is "damaged" as soon as a single one of the k stocks it needs is unavailable. Therefore, in the long-time limit, for $1 \ll \tau_{\max} \ll k \ll N$, the average velocity of the hour-hand is negligible, and most of the region between the origin and the minute-hand position, $i_{\min}(t)$, is occupied by impaired firms. In other words, and mixing metaphors, the long-term dynamics is dominated by the "hare" that outruns the "tortoise."

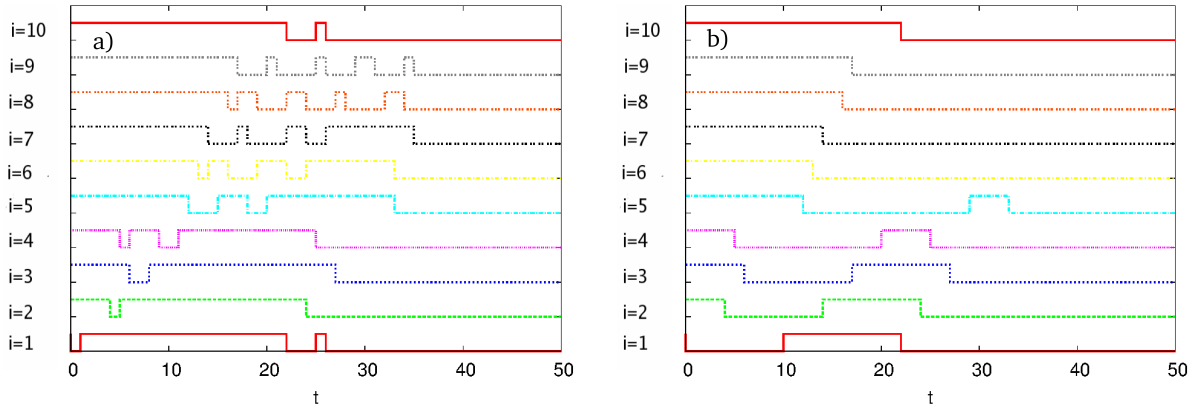

Fig. 5. Time evolution of the state of the 10 nodes of the asynchronous free model on a braid chain, with $k = 2$, after an initial perturbation of node 1. Same plotting convention as in [Fig. 2] and [Fig. 4]. (a) The duration of the initial perturbation is $\tau_c = \tau_{\min} = 1$ day; and (b) $\tau_c = \tau_{\max}$. This yields transients of length 35 days and 33 days, respectively.

In this limit, one can evaluate rather accurately how far the hare goes in one time step $\tau_{\min} = 1$, i.e., the approximate average velocity v^* of the signal from a given supplier j to its farthest customer i for which $\tau_{ij} = 1$. At most, the signal can travel up to $i = j+k$ with probability $\mathcal{P}(\tau_{j+k,j} = 1) = 1/\tau_{\max}$. Generally, the probability that it moves a distance at most l is obtained by taking $\tau_{h,j} > 1$ for $h = j+k, j+k-1, \ldots, j+l+1$ and $\tau_{j+l,j} = 1$. To get the average distance, one has to sum all possible values $l = 0, 1, \ldots, k$, multiplied by the corresponding probability. Here $i = j + l$ is the farthest reachable point, and it follows that

$$v^* = \sum_{l=0}^{k} \frac{l}{\tau_{\max}} \left(1 - \frac{1}{\tau_{\max}}\right)^{l-k} \simeq k - (\tau_{\max} - 1), \tag{18}$$

where we used the two identities

$$\sum_{l=0}^{\infty} \epsilon^l = \frac{1}{1-\epsilon},$$
$$\sum_{l=0}^{\infty} l\, \epsilon^l = \epsilon\, \frac{d}{d\epsilon} \frac{1}{(1-\epsilon)}, \tag{19}$$

with $\epsilon = (1 - 1/\tau_{\max})$. The result in Eq. (18) is still an underestimate for the effective average velocity in the long-time limit, since we have neglected here corrections of order ϵ^k that augment v further. Moreover, we have also omitted the fact that signal can go even faster in more than one time step.

Still, we get fairly accurate bounds on the average signal velocity v:

$$k - (\tau_{\max} - 1) \leq v \leq k - 1; \tag{20}$$

here the lower bound $v_{\min} = v^*$ is obtained by using the hare argument, while the upper one, $v_{\max}$, results from the particular case in which all the delays equal $\tau_{\min}$. Based on the form of both these estimates, we expect the average density $\langle \rho(t, \mathcal{T}) \rangle$ to be approximately linear in time, with $1 - (1/N) - v_{\max} t/(N-1) < \langle \rho(t, \mathcal{T}) \rangle < 1 - v_{\min} t/N$. Numerical results are presented in [Fig. 6] and are in good agreement with this expectation.

A different approach is worked out in Appendix B, where the average number of impaired firms is explicitly computed as a function of the probability for the signal to have propagated by l positions in t time steps, cf. Eq. (61). This analysis confirms that the average density is linear over a large time window, and it allows us to predict the effective slope.

In [Fig. 6], we also consider delays that depend only upon the customers, $\tau_{ij} = \tau(i)$, or only upon the suppliers, $\tau_{ij} = \tau(j)$; here $\{\tau(i) : 1 \leq i \leq N\}$ and $\{\tau(j) : 1 \leq j \leq N\}$ are, as usual, uniformly distributed in the interval $[\tau_{\min}, \tau_{\max}]$. We get the same, slightly slower, average signal velocity in these last two cases.

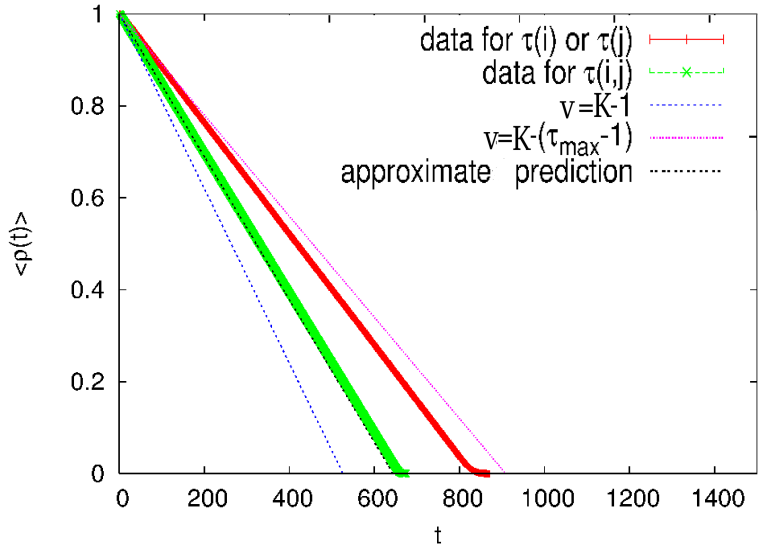

Fig. 6. The average density $\langle \rho(t, \mathcal{T}) \rangle$ as a function of time, in the asynchronous free model on a braid chain, after an initial perturbation of node 1 of duration $\tau_c = \tau_{\min}$. The network size is $N = 10\,000$, and the in/out-degree is $k = 20$; the average is taken over $\mathcal{N}_s = 100$ different configurations $\mathcal{T}$ of the delays. The legend distinguishes between delays that (i) depend only upon the customer, $\tau_{ij} = \tau(i)$; (ii) only upon the supplier, $\tau_{ij} = \tau(j)$; and (iii) upon both of them, $\tau_{ij} = \tau(i, j)$. We compare the numerical results with the lower and upper bounds on the linear behavior, $k - (\tau_{\max} - 1) \leq v$ and $v \leq k - 1$, cf. Eq. (20), and with the approximate prediction of Eq. (61) in Appendix B. See text for details.

This slowing down can be qualitatively explained by the observation that there is a smaller number of propagation paths of different time lengths and thus less of an opportunity for a "runaway hare."

We checked that the observed linear decay in the density of healthy sites and the agreement with the theoretical expectations do not depend upon the particular choice of model parameters. Moreover, as soon as $\tau_c \geq \tau_{\min}$, the average density only depends upon τ_c roughly during the first τ_c time steps. Clearly, these results imply that $\langle \rho_\infty(\mathcal{T}) \rangle = 0$ in the present model as soon as $\tau_c \geq \tau_{\min}$, and that the average transient $\langle T_0(\mathcal{T}) \rangle = \langle T_\varpi(\mathcal{T}) \rangle$ is bounded between approximately $(N-1)/(k-1)$ and $\sim N/[k - (\tau_{\max} - 1)]$.

On the other hand, for $\tau_c < \tau_{\min}$, one finds the same kind of asymptotic solution as in the previously considered synchronous free model with $k \geq 2$. Namely, for $\tau_c < \tau_0$, one obtains only periodic solutions of period $\varpi = \tau_{\min}$, with all the firms simultaneously impaired in the first part of the period, of length τ_c. In fact, this peculiar kind of asymptotic solutions can appear also for $\tau_{\min} \leq \tau_c < \tau_{\max}$, since there are configurations $\mathcal{T}$ of the delays in which the shortest nearest-neighbor propagation path is $\tau^*(\mathcal{T}) > \tau_c$, and the argument given in Section 3.4 does apply. Nevertheless, as already noted there, the probability of such a set $\mathcal{T} = \{\tau_{ij}\}$ rapidly approaches zero for increasing N values.

3.6. *Forced braid-chain models with* $k = 1$

We now turn to the study of forced models on a braid chain with in/out-degree $k = 1$, as defined in Eq. (13). When the updating is synchronous, the equation for each x_i reduces to

$$x_i(t) = \left\{ \sum_{j=0}^{N-1} \overline{x}_{i-j} \left[t - (j+1)\tau_0 \right] \right\} \vee x_i(t - N\tau_0); \tag{21}$$

the sum here refers to Boolean addition, *i.e.* to the Boolean OR operator $\vee$. For asynchronous updating the resulting equation becomes

$$x_i(t) = \left[\sum_{h=0}^{N-1} \overline{x}_{i-h} \left(t - \sum_{j=0}^{h} \tau_{i-j,i-j-1} \right) \right] \vee x_i \left(t - \sum_{j=0}^{N-1} \tau_{i-j,i-j-1} \right), \tag{22}$$

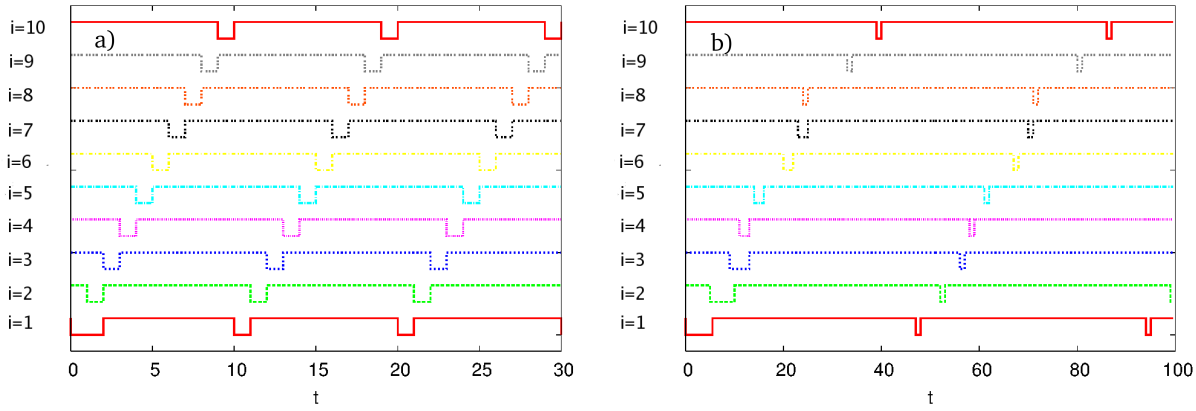

Fig. 7. Time evolution of the state of the 10 nodes of a forced model on a braid chain, with $k = 1$, after an initial perturbation of node 1. Same plotting convention as in [Fig. 2] and other similar figures: (a) synchronous, and (b) asynchronous case. The duration of the initial perturbation is taken to be $\tau_c = 2\tau_0 = 2$ days and $\tau_c = \langle \tau_{ij} \rangle = 5.5$ days, respectively; hence the solutions are not periodic right away in either case. See text for details.

with the propagation times along the paths given by the corresponding sums of random τ_{ij}'s.

The models' dynamical behavior differs according to whether:

- The initial perturbation's duration, τ_c, is shorter than or equal to the shortest nearest-neighbor propagation path, which in turn means that:

  – $\tau_c \leq \tau_0$ in the synchronous model; or
  – $\tau_c \leq \tau^*(\mathcal{T})$ in the asynchronous one. Note that the probability of $\tau^*(\mathcal{T}) > \tau_{\min}$ becomes rapidly negligible in the limit of large N.

  In this case, the solutions are immediately periodic, like those of the corresponding free models of Sections 3.2 and 3.3; see again [Fig. 2]. One observes a wave of nodes that take the value zero, for a duration τ_c, one after the other; this wave propagate across the spatio-temporal pattern. The period ϖ is given by the sum of the delays along the whole chain, namely:

  – $\varpi = N\tau_0$ for equal delays; and
  – $\varpi(\mathcal{T}) = \sum_{i=1}^{N} \tau_{i,i-1}$, with $\langle \varpi(\mathcal{T}) \rangle = N(\tau_{\max} + 1)/2$, for randomly selected ones.

- The initial-damage duration τ_c is longer than the shortest nearest-neighbor propagation path, *i.e.* $\tau_c > \tau_0$ or $\tau_c > \tau^*(\mathcal{T})$ in the synchronous and asynchronous model, respectively. As shown in [Fig. 7], the solutions here become periodic only after a transient $T_0 > 0$: when the firm in position i is reached by the wave of damage, its activity is affected for a duration that lasts:

  – no longer than τ_0, for equal delays; and
  – no longer than $\tau_{i,i-1}$, for randomly selected ones.

  Hence the transient is short for equal delays — one finds $T_0 = T_\varpi \simeq \tau_c$ — whereas it can be of the order of the time that the wave takes to propagate across the whole network, *i.e.* of the period ϖ of the solution, for randomly selected ones. The asymptotic periodic solutions are the same:

  – as for $\tau_c = \tau_0$ in the synchronous model; and
  – as for $\tau_c = \tau^*(\Omega)$ in the asynchronous one.

  Note that the asymptotic density ρ_∞ equals 1 in the large-N limit in all of these cases, with corrections of order $1/N$, as in the corresponding free models.

3.7. *Synchronous forced model with $k \geq 2$*

The behavior of the forced model on a braid chain, with in/out-degree $k \geq 2$, can be described in detail when the delays are all equal to τ_0; Eq. (13) then becomes:

$$x_i(t) = \overline{x}_i(t - \tau_0) \vee \left[\prod_{j=1}^{k} x_{i-j}(t - \tau_0) \right] . \tag{23}$$

In this case, the firm i maintains its production, as usual, if all its suppliers were fully functional at the previous time step, but also if some of them were impaired and i itself was impaired during the previous time interval: the production is thus recovered after one time step of length τ_0, thanks to the external input.

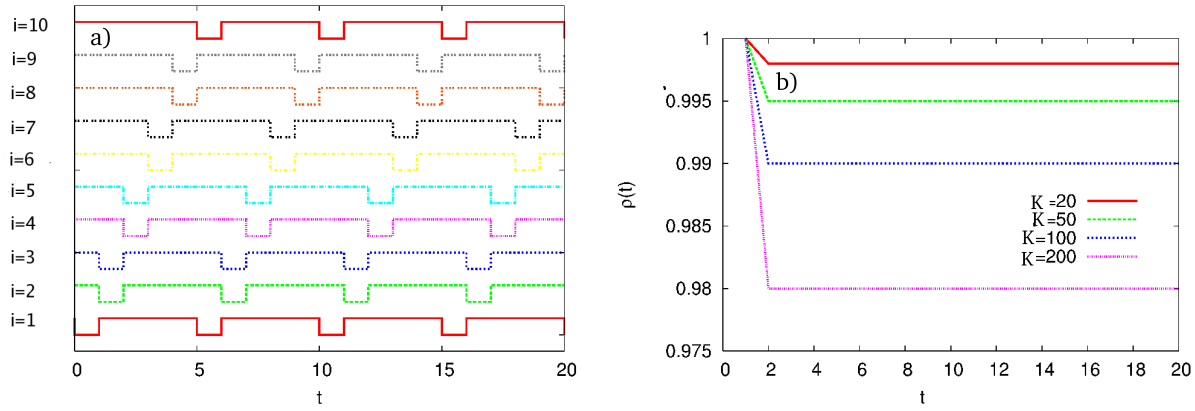

Fig. 8. (a) Time evolution of the state of the $N = 10$ nodes of the synchronous forced model on a braid chain, with $k = 2$, after an initial perturbation of node 1; same plotting convention as in [Fig. 2] and other similar figures. (b) Density $\rho(t)$ as a function of time in the same type of model, for a network size of $N = 10\,000$; the values $k = 20, 50, 100, 200$ of the in/out-degree are given in the panel legend. In both panels, we take a duration of the initial damage of $\tau_c = \tau_0 = 1$ day.

Let us take for simplicity N equal to a multiple of k, and a duration of the initial perturbation of $\tau_c = \tau_0$. After the first time step, there are k firms in consecutive positions along the chain whose activity is simultaneously impaired; at the subsequent time step, these firms recover but the damage propagates to the next k firms.

In other words, in this model, as soon as $t > 1$, both the hour-hand and the minute-hand move with the same constant velocity $v = k$: the damage does not spread, but the activity never recovers completely. Correspondingly, the asymptotic solution is periodic right away, with period $\varpi = N/k$, and the density is constant, $\rho(t) = \rho_\infty = 1 - k/N$, as illustrated in [Fig. 8].

For $\tau_c > \tau_0$, the behavior is the same, apart from the fact that the solutions are not periodic right away: there is a very short transient $T_0 \simeq \tau_c$ in this case. For $\tau_c < \tau_0$, one still finds a propagating wave of k impaired firms in consecutive positions along the chain; nevertheless, their activity is simultaneously impaired only in the first part, having length τ_c, of the time step. The situation is similar to the one encountered in the same case in free models, *i.e.* it is the behavior of the initially impaired firm that propagates across the network, cf. Eq. (17).

While no complete breakdown of the economy occurs, the comparison of the results in this subsection with the previous Section 3.6 clearly shows that higher connectivity in a production chain can lead to a less favorable outcome, with more firms being impaired in the long run. This result can be explained by the fact that — at least for the present model formulation — a larger number of connections does not lead to risk sharing, since a single impaired supplier suffices to stop a firm's production. This assumption amounts to saying that each supplier provides a different type of goods or services to a given firm, and that one of its suppliers cannot compensate for the loss of another one. In such a situation, a firm that depends on

several suppliers has a higher risk of being indirectly affected by a shock, whether natural or man-made.

3.8. *Asynchronous forced model with $k \geq 2$*

In the presence of randomly selected delays, external intervention on a braid chain with $k \geq 2$ in/out-degree renders model behavior considerably more complex. The solution for a typical set of delays $\mathcal{T}$, after an initial perturbation of duration $\tau_c = \tau_{\min}$, is shown in [Fig. 9]: intriguingly, despite the relatively small network size $N = 10$ and the small degree $k = 2$ under consideration, no periodicity is reached over the fairly long time intervals studied.

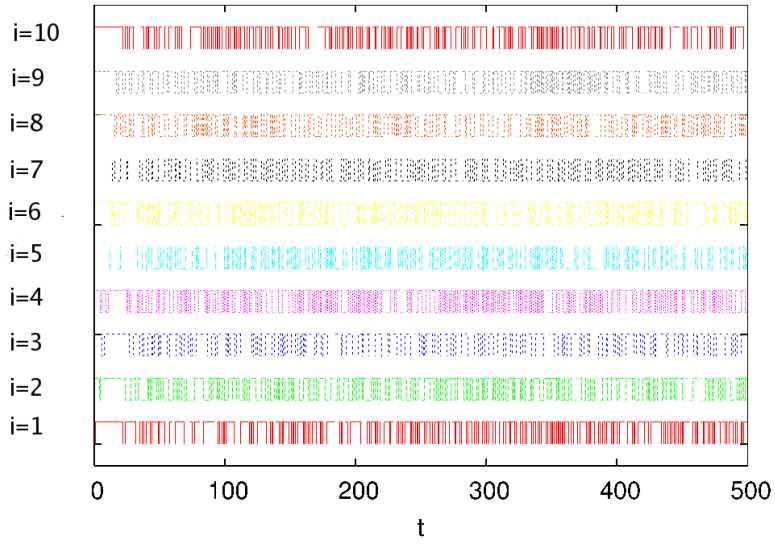

Fig. 9. Time evolution of the state of the 10 nodes of the random forced model on a braid chain, with $k = 2$, after an initial perturbation of node 1. Same plotting convention as in [Fig. 2] and in other similar figures. As usual, we look at a typical configuration $\mathcal{T}$ of randomly selected delays, uniformly distributed between $\tau_{\min}$= 1 day and $\tau_{\max}$=10 days. The duration of the initial perturbation is $\tau_c = \tau_{\min}$. Notice that the solution does not display any periodicity in the fairly long time window displayed.

Since the delays are integer multiples of $\tau_{\min}$, the asymptotic solution of system (2), for a given set of delays $\mathcal{T}$ is either constant or periodic, because of mathematically rigorous results on BDEs [Ghil *et al.*, 2008; Mullhaupt, 1984; Ghil & Mullhaupt, 1985]. Nevertheless, for irrationally related delays, BDEs can have solutions of increasing complexity, which display a number of jumps per unit time that increases polynomially with time. Such peculiar behavior occurs, in particular, in the case of conservative systems with rationally unrelated delays.

This behavior is exemplified, at its simplest, by the scalar BDE [Dee & Ghil, 1984; Ghil & Mullhaupt, 1985]

$$x(t) = x(t - \tau) \bigtriangledown x(t - 1), \tag{24}$$

where $\tau \in (0, 1)$ is irrational, and $\bigtriangledown$ is the 'XOR' operator, for which $x \bigtriangledown y = 1$ iff $x \neq y$. An aperiodic solution obtained with a set $\mathcal{T}_{\text{irr}}$ of delays can be approximated with prescribed accuracy, for increasingly long times, by the periodic solutions of nearby BDEs systems with the same Boolean operators but with rationally related sets of delays $\mathcal{T}_n$. The latter approximate better and better the former, as $\mathcal{T}_n \to \mathcal{T}_{\text{irr}}$ [Ghil *et al.*, 2008; Ghil & Mullhaupt, 1985].

Though a more careful analysis would be necessary in order to extend these results to the present case,

we notice that Eq. (13), which describes our forced models on a braid chain, is equivalent to:

$$\overline{x}_i(t) = \sum_{j=1}^{k} x_i(t_{ij}) \bigtriangledown \overline{x}_{i-j}(t_{ij}) \bigtriangledown [\overline{x}_i(t_{ij}) \cdot x_{i-j}(t_{ij})] \tag{25}$$

where we defined $t_{ij} := t - \tau_{i,i-j}$. The equivalence is due to the Boolean relations $\overline{a \vee b} = \overline{a} \wedge \overline{b} = \overline{a} \bigtriangledown \overline{b} \bigtriangledown (\overline{a} \cdot \overline{b})$, and it shows that the system under consideration is *partially linear* in the BDE terminology of [Ghil *et al.*, 2008; Ghil & Mullhaupt, 1985], *i.e.* that it contains a conservative subsystem. This suggests that the model might approximate, with an accuracy depending on the particular $\mathcal{T}$-configuration, similar sets of BDEs with delays that are incommensurable, and whose solutions thus display chaotic behavior.

In order to better characterize our numerical findings, we numerically study the following three quantities: the transient $T_\varpi(\mathcal{T})$; the period $\varpi(\mathcal{T})$ of the asymptotic solution; and the period-averaged asymptotic density $\rho_\infty(\mathcal{T})$ of fully active firms. According to Eq. (8),

$$\rho_\infty(\mathcal{T}) = \frac{1}{\varpi} \int_{T_\varpi}^{T_\varpi + \varpi} \rho(t, \mathcal{T}) \mathrm{d}t, \tag{26}$$

where $T_\varpi = T_\varpi(\mathcal{T})$ and $\varpi = \varpi(\mathcal{T})$. Notice that — in the models considered so far, and in particular in the free models with $k \geq 2$ studied in Sections 3.4 and 3.5 — $T_\varpi(\mathcal{T}) = T_0(\mathcal{T})$, where $T_0(\mathcal{T})$ is the time that the density $\rho(t, \mathcal{T})$ takes to reach the asymptotic value $\rho_\infty(\mathcal{T})$.

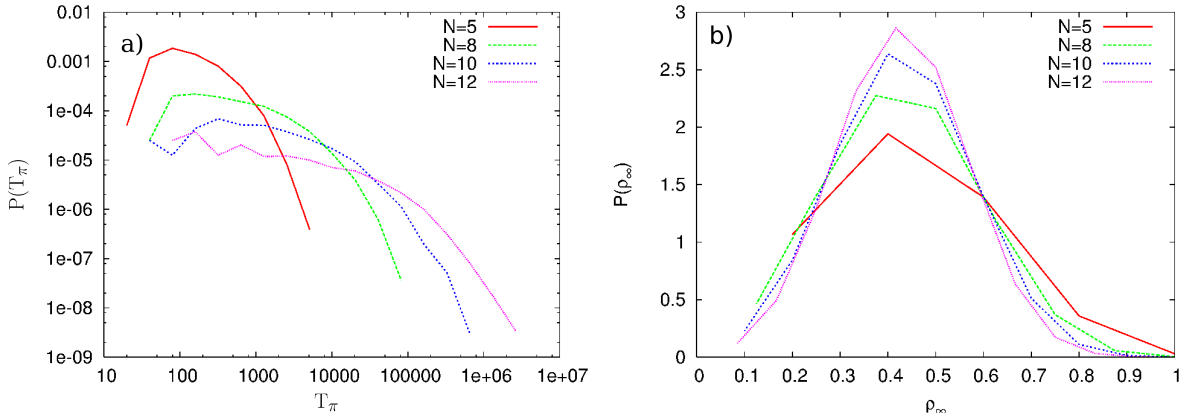

Fig. 10. Probability distributions for the asynchronous forced model on a braid chain with $k = 2$. The results pertain to the solutions of small systems of $N = \mathcal{O}(10)$ equations, and are obtained from $\mathcal{N}_s = 1000$ different sets of delays $\mathcal{T}$. (a) Probability distribution $\mathcal{P}(T_\varpi(\mathcal{T}))$ of the transient; (b) probability distribution $\mathcal{P}(\rho_\infty(\mathcal{T}))$ of the period-averaged asymptotic density of "healthy" firms. Panel (a) uses log-log coordinates, in order to emphasize that the probability $\mathcal{P}(T_\varpi(\mathcal{T}))$ is still significant even at very large values. See text for details.

These quantities can be determined with high accuracy for relatively small system sizes $N \lesssim 12$. We present in [Fig. 10] our results on the probability distributions $\mathcal{P}(T_\varpi(\mathcal{T}))$, and $\mathcal{P}(\rho_\infty(\mathcal{T}))$, as obtained by considering $\mathcal{N}_s = 1000$ sets $\mathcal{T}$ of random delays; the behavior of $\mathcal{P}(\varpi(\mathcal{T}))$ is very similar to the one displayed by $\mathcal{P}(T_\varpi(\mathcal{T}))$.

The most striking feature in the figure is that both the transient $T_\varpi(\mathcal{T})$ and the period $\varpi(\mathcal{T})$ of the solutions can increase very rapidly with the network size N. In order to better visualize this, we have plotted $\mathcal{P}(T_\varpi(\mathcal{T}))$ on a log-log scale in [Fig. 10a]) and find that — in systems of $N = 12$ nodes — it is not vanishingly small even for values of the transient $T_\varpi(\mathcal{T})$ as large as 10^6 (in units of $\tau_{\min}$).

Actually, we found that the average length of the transient diverges exponentially with N, $\langle T_\varpi(\mathcal{T}) \rangle \propto \exp(\mathrm{const} \cdot N)$, and that, at least for the N values under consideration, the average period $\langle \varpi(\mathcal{T}) \rangle$ displays a similar behavior. Such an exponential increase is also characteristic of the so-called chaotic regime observed in random Boolean networks [Drossel, 2008; Kauffman, 1993; Weisbuch, 1991], in which the delays are all equal, but it is the link configuration Ω that is randomized.

The probability distribution $\mathcal{P}(\rho_\infty(\mathcal{T}))$ of the asymptotic density $\rho_\infty(\mathcal{T})$ of fully active firms, averaged over the $\mathcal{T}$-dependent period $\varpi(\mathcal{T})$, is shown in [Fig. 10b] for several values of $N \leq 12$. It turns out to be roughly bell-shaped, and it becomes more peaked around the mean value as the network size N increases. This increase in concentration around the mean suggests that the fairly complex dynamics does not imply a more unpredictable behavior of macroscopic intensive quantities, at least in the limit of large N (not shown).

In fact, whereas to predict a given solution's detailed evolution in time for a given set $\mathcal{T}$ of random delays seems to be quite hard, one can use the "two-handed clock" approach, as in Section 3.5, to obtain the expected behavior of various average quantities. For simplicity, we limit the analysis to the case in which the duration τ_c of the initial damage exceeds the length $\tau^*(\mathcal{T})$ of the smallest nearest-neighbor propagation path, where $\tau^*(\mathcal{T})$ is usually equal to $\tau_{\min}$. In this case, we do not expect to encounter short-periodic asymptotic solutions with all the firms being simultaneously down in the first part of the period.

Since the network is a braid chain and the production of a given firm, apart from the initially damaged one, is impaired for the first time as soon as one of the k stocks that it needs is unavailable, the hare argument can still be used for obtaining a close upper bond on the average signal velocity v. Hence we argue that, in the limit $1 \ll \tau_{\max} \ll n \ll N$, and at large t, the signal that propagates across the chain with the average velocity v is still well approximated by Eq. (18), *i.e.* $v \lesssim v^* = k - (\tau_{\max} - 1)$.

The main difference with respect to the previous asynchronous free model is that here, because of the external-rescue inputs, only a fraction s of the firms between the origin and the minute-hand position is impaired on average, during a time step of length $\tau_{\min}$. Since the delays are independently and identically distributed along the whole chain, at large enough times this fraction s is constant, and the damage spreads linearly with time, up to the point of invading the whole network, according to:

$$\langle \theta(t) \rangle \simeq \begin{cases} sNvt \lesssim sNv^*t = sN[k - (\tau_{\max} - 1)]t, & \text{for } 1 \ll t \lesssim \langle T_0^*(\mathcal{T}) \rangle, \\ sN, & \text{for } t \geq \langle T_0^*(\mathcal{T}) \rangle; \end{cases} \tag{27}$$

with

$$\langle T_0^*(\mathcal{T}) \rangle \simeq \frac{N}{v} \gtrsim \frac{N}{v^*} = \frac{N}{k - (\tau_{\max} - 1)}. \tag{28}$$

The average density of fully active firms, $\langle \rho(t; \mathcal{T}) \rangle = 1 - \langle \theta(t; \mathcal{T}) \rangle / N$ is thus decreasing again linearly, and the negative slope is approximated by $-v^*$, up to the time $\langle T_0(\mathcal{T}) \rangle$ at which it reaches the nearly constant asymptotic value $\langle \rho_\infty(\mathcal{T}) \rangle \simeq 1 - s$.

Hence, the *effective transient* $\langle T_0(\mathcal{T}) \rangle$ refers to the dynamics of $\langle \rho(t; \mathcal{T}) \rangle$; in fact, it is the time at which the minute-hand reaches the origin again, after a whole tour: it is therefore of the same order as the time that the density takes to reach the asymptotic zero value in the asynchronous free model. It is clearly important to distinguish between the transient $T_\varpi(\mathcal{T})$, defined as the time elapsed before periodicity settles in — which increases on average exponentially with network size N — and the definitely shorter effective transient time $\langle T_0(\mathcal{T}) \rangle$. The latter can be more generally defined as the time at which macroscopic observables approach nearly constant values.

We present in [Fig. 11] a single-sample density, $\rho(t; \mathcal{T})$, as a function of time — and, as usual, after an initial perturbation of node 1 of duration $\tau_c = \tau_{\min}$ — for a large network size $N = 10\,000$ and in/out-degree $k = 20$. In agreement with the picture emerging from the previous discussion, we find small fluctuations around a linear decay, followed by small fluctuations around the asymptotic value, $\rho_\infty(\mathcal{T}) \simeq 0.15$. The latter is reached in a time $T_0^*(\mathcal{T}) \simeq 650$ (in $\tau_{\min}$ units), which compares favorably with the estimate of the average effective transient, $\langle T_0(\mathcal{T}) \rangle \lesssim 900\tau_{\min}$ that one gets from Eq. (28).

The numerical results are for a single, typical set of delays $\mathcal{T}$. For large enough N-values, we find that the fluctuations of $\rho(t; \mathcal{T})$ around the average value $\langle \rho(t; \mathcal{T}) \rangle$ are usually very small, *i.e.* $\rho(t; \mathcal{T}) \simeq \langle \rho(t; \mathcal{T}) \rangle$: in fact, they are usually of the same order of magnitude as the fluctuations of the single-sample density $\rho(t; \mathcal{T})$ around the constant asymptotic value displayed in the present plot. This finding is in agreement with the behavior of $\mathcal{P}(\rho_\infty(\mathcal{T}))$ shown in [Fig. 10b] and it can generally be expected for a macroscopic intensive quantity, such as the density. We checked in particular that both the effective transient $T_0^*(\mathcal{T})$ and the asymptotic average value of the density, $\rho_\infty(\mathcal{T}) \simeq 1 - s$, are usually almost indistinguishable for different choices of the randomly selected set of delays $\mathcal{T}$.

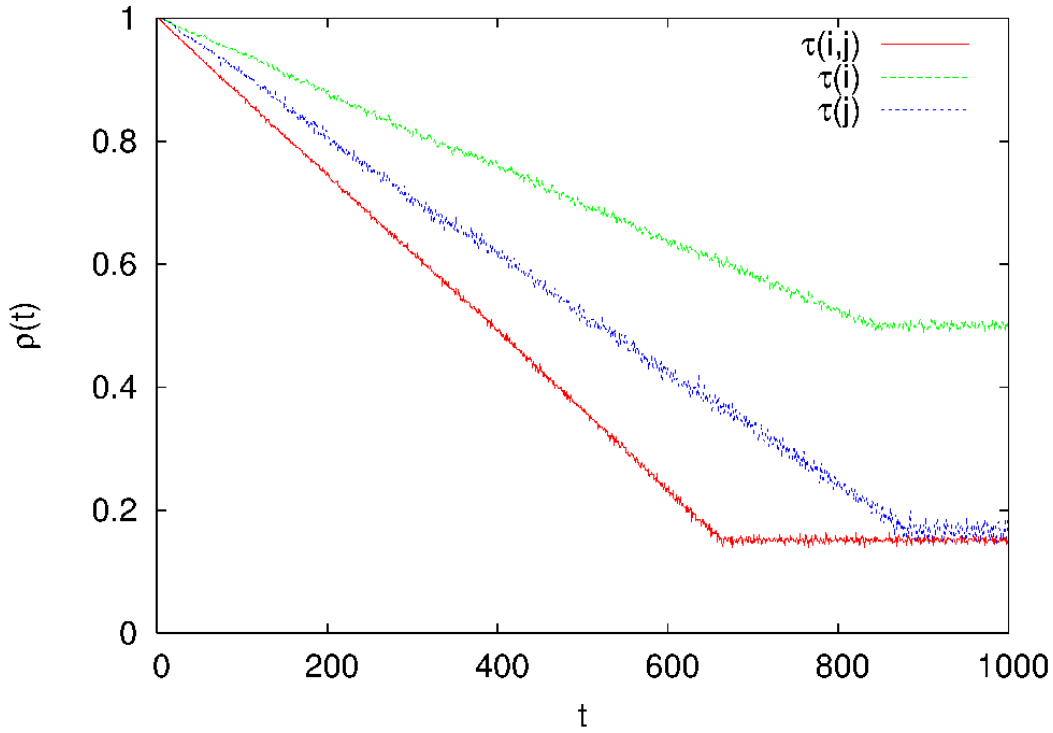

Fig. 11. Evolution of the density $\rho(t, \mathcal{T})$ of fully active firms as a function of time for a typical set of delays $\mathcal{T}$, in the asynchronous forced model on a braid chain, after an initial perturbation of node 1 of duration $\tau_c = \tau_{\min} = 1$ day. The network size is $N = 10\,000$ and the in/out-degree is $k = 20$. We study delays $\tau_{ij} = \tau(i)$ that depend only on the customers; delays $\tau_{ij} = \tau(j)$ that depend only on the suppliers; and delays $\tau_{ij} = \tau(ij)$ that depend on both of them. See text for details.

Besides considering delays $\{\tau_{ij}\}$ that depend upon both the customer i and the supplier j (red curve in the figure), we present in [Fig. 11] also numerical results on the single-sample density $\rho(t; \mathcal{T})$ for models whose delays depend only upon the customers, $\tau_{ij} = \tau(i)$ (green curve), or only upon the suppliers, $\tau_{ij} = \tau(j)$ (blue curve). In the latter two cases, the effective transient times $T_0^*(\mathcal{T})$ are roughly equal, and definitely longer than in the first case. The faster decay in the latter case (red curve) can be explained by noticing that — as in the asynchronous free model studied in Section 3.5 — when τ_{ij} depends upon both its indices, there are more concurrent propagation paths of different durations in the system, hence the average signal propagation velocity is higher.

The constant asymptotic mean value of the density, $\rho_\infty(\mathcal{T}) \simeq 1 - s$, is definitely larger when the delays depend only upon the customers (green curve), whereas it is almost the same for the other two cases (blue and red curves). In fact, when $\tau_{ij} = \tau(i)$, Eq. (13) becomes:

$$x_i(t) = \overline{x}_i[t - \tau(i)] \vee \left\{ \prod_{j=1}^{k} x_{i-j}[t - \tau(i)] \right\} . \tag{29}$$

Hence, there is a definitely smaller number of delay combinations $\mathcal{T}$ that can result in affecting the production of a given firm, *i.e.* the average fraction s of simultaneously impaired firms — within the region reached by the spreading of the initial perturbation — is smaller. In fact, Eq. (29) implies that, after the transient $T_0^*(\mathcal{T})$, when averaging the dynamics over a large enough time interval, each firm is impaired roughly for one half of the time; equivalently, for large $N \gg k$, there is, on average, one half of the firms that are impaired at each time step, *i.e.* $s \simeq 0.5$. This is in perfect agreement with the result on the asymptotic value of the density, $\rho_\infty(\mathcal{T}) \simeq 0.5$, that one finds in [Fig. 11] for $\tau_{ij} = \tau(i)$ (green curve).

To summarize, the external rescue inputs in the forced model on a braid chain do prevent economic collapse, *i.e.* one finds a nonzero fraction of fully active firms in the large-time limit. This fraction can be

as large as one half of the total number of firms, whereas the collapse of the production chain is total in the absence of such external inputs, cf. [Fig. 6].

4. Directed random graphs (DRGs)

4.1. *Network topology*

The study of BDEs for the relatively simple topology of braid chains — with their geometric periodicity and strong connectivity — held considerable interest for two reasons: (i) it allowed us to compare numerical results with analytical considerations; and (ii) it provided a first glimpse at the substantial differences between free and forced models, on the one hand, and between synchronous and asynchronous forcing, on the other.

We now shift our attention to the more realistic topology of DRGs. Here the elements of the connectivity matrix A are given by Eq. (1) and we start by a quick review of the well known features of such a random structure [Karp, 1990; Łuczac & Seierstad, 2009].

P. Erdős and A. Rényi initiated the study of random graphs about 50 years ago [Erdős & Rényi, 1959, 1960, 1961]; such graphs have been extensively studied more recently, along with a number of related models [Bollobás, 1998; Watts, 1999; Albert & Barabási, 2002; Newman, 2003]. One gets an undirected Erdős-Rényi random graph $G(N, p)$ by taking the edges that connect each possible pair (i, j) of the N nodes to be independently and identically distributed with probability p. In our notation, the matrix A is symmetric, since the event $A_{ij} = 1$ implies the event $A_{ji} = 1$, and vice-versa.

The total number of pairs of nodes is $N(N-1)/2$, and each edge contributes to the degree of the 2 nodes that are its endpoints; the average connectivity z is given, therefore, by $z = \langle k \rangle = (N-1)p \simeq Np$. The probability distribution of the degree k is, in fact, binomial:

$$\mathcal{P}(k) = \binom{N-1}{k} p^k (1-p)^{N-1-k} \simeq \frac{z^k}{k!} e^{-z}, \tag{30}$$

and it converges to a Poisson distribution with mean $z = \langle k \rangle$ in the limit of large N and small p.

One defines *a connected component* $\mathcal{S}_c$ of the graph as an ensemble of nodes such that, from each node $i \in \mathcal{S}_c$, there exists at least one path $\mathcal{C}_{ij}$ — across nodes $\{h_1, h_2, \ldots, h_l\}$ belonging to the same $\mathcal{S}_c$ — that reaches each other possible node j in that $\mathcal{S}_c$:

$$\forall (i, j) \in \mathcal{S}_c \Rightarrow \exists\, \mathcal{C}_{ij} : A_{ih_1} A_{h_1 h_2} \cdot \ldots \cdot A_{h_l j} \neq 0 \qquad h_1, h_2, \ldots, h_l \in \mathcal{S}_c. \tag{31}$$

The average size S_c of a connected component $\mathcal{S}_c$ can, therefore, be evaluated by starting from a randomly chosen node, and computing the number of its first neighbors z_1, of its second neighbors z_2, and so on. For the simple case of a Poisson distribution, one has:

$$\begin{aligned} z_1 &= \sum_{k=0}^{\infty} k \frac{z^k}{k!} e^{-z} = z\,, \\ z_2 &= \sum_{k=0}^{\infty} k(k-1) \frac{z^k}{k!} e^{-z} = z^2\,, \\ z_l &= \frac{z_2}{z_1} z_{l-1} = \left(\frac{z_2}{z_1}\right)^{l-1} z_1 = z^l\,; \end{aligned} \tag{32}$$

hence one obtains:

$$S_c = \sum_{l=0}^{\infty} z^l = \frac{1}{1-z} \text{ for } z < 1. \tag{33}$$

In the $N \to \infty$ limit, one thus finds that $\langle S_c \rangle$ diverges as $z \to z_c = 1$. Above this *critical value* $z_c = 1$, a giant connected component $\mathcal{S}_{gc}$ appears, and $\mathcal{S}_{gc}$ contains a finite fraction $0 < s_{gc} \leq 1$ of the nodes, $S_{gc} = s_{gc} N$, as usually observed in real networks. This "phase transition" was already enphasized in the

pioneering papers of Erdős and Rényi [Erdős & Rényi, 1959, 1960, 1961], and was subsequently studied in great detail from both the mathematical [Bollobás, 1998] and the physical point of view [Albert & Barabási, 2002].

When z exceeds 1, $s_{\rm gc}$ tends rapidly towards 1. Let us call r the fraction of nodes that do not belong to the giant connected component $\mathcal{S}_{\rm gc}$, $r = 1 - s_{\rm gc}$. The value of r is obtained by observing that such nodes have successive neighbors not belonging to this giant component. Based on the Poisson process equations, we get

$$r = \sum_{l=0}^{\infty} \frac{[zr]^l}{l!} e^{-z} = e^{z(r-1)}. \tag{34}$$

This result can also be derived in the probabilistic framework of generating functions [Newman *et al.*, 2001], a framework that is well suited for applications to more general distributions $\mathcal{P}(k)$ of the degree k, as well as to DRGs, and is presented in Appendix C.

In fact, the DRG $D(N,p)$ that we are considering is a simple generalization of the Erdős-Rényi model, except that we have to distinguish between the number $k_{\rm in}$ of in-links and the number $k_{\rm in}$ of out-links. Still, each directed link is chosen independently with the same probability p among the $N(N-1)$ possible ones. Hence the average in/out-degree $z = \langle k \rangle = \langle k_{\rm in} \rangle = \langle k_{\rm out} \rangle$ is again given by $\langle k \rangle = (N-1)p \simeq Np$, and $\mathcal{P}(k_{\rm in}) = \mathcal{P}(k_{\rm out})$ are still described by Eq. (30). Notice that — if we were to transform a DRG into an undirected graph, by interpreting each link as an edge — we would get a random graph with average degree equal to twice the average in/out-degree of the DRG we started with.

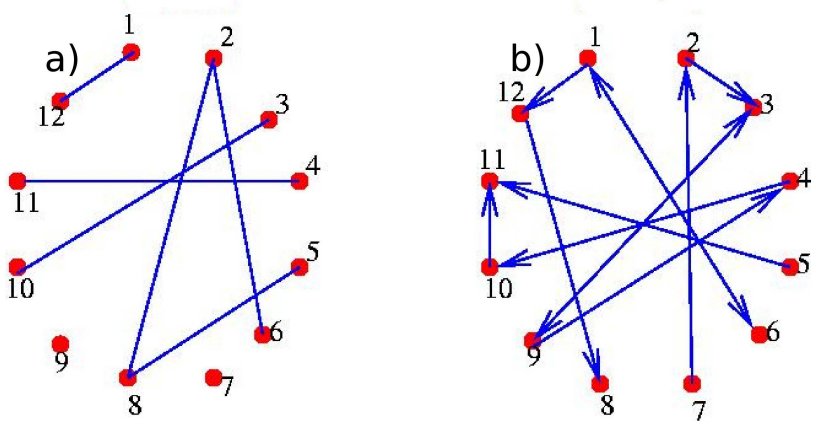

Fig. 12. Typical realizations (a) of a random (undirected) graph $G(N,p)$, and (b) of a directed random graph (DRG) $D(N,p)$. The two graphs have the same small network size of $N = 12$ nodes, and the same $p \simeq 1/N$ and $\langle k \rangle \simeq 1$ value for both. The number of the edges in the random graph is one half the number of the directed links in the DRG.

We illustrate in [Fig. 12] the differences between a typical undirected random graph $G(N,p)$ in the left panel and a DRG $D(N,p)$ in the right panel. Both graphs have the same number $N = 12$ of nodes, and the same values $p \simeq 1/N$ and $\langle k \rangle \simeq 1$. It is clear from this figure how different the random topology is from that of the brain chain. In the latter, and for the same in/out-degree value $k = 1$, one would find a single connected component of size N (see again [Fig. 1]). Instead, in [Fig. 12] here — and looking for simplicity at the left panel — we observe two isolated nodes, three connected components of size 2, and one connected component of size 4.

It is likewise clear from the figure that, in the directed case [Barbosa *et al.*, 2003; Newman *et al.*, 2001; Dorogovtsev *et al.*, 2001; Broder *et al.*, 2000], the existence of a path that connects i to j does not usually imply the existence of a path connecting j to i. For each given node, one can hence define:

- the out-component, which is the set of all nodes that can be reached from it;
- the in-component, which is the set of all nodes from which it can be reached;

- the strongly connected component, which is the set of all the nodes that can be reached from it *and* from which it can be reached, *i.e.* the intersection of the in-component and the out-component; and, finally,
- the weakly connected component, which is the set of all the nodes that can be reached from it *or* from which it can be reached, *i.e.* this component is the union of the in-component and the out-component.

The weakly connected component also corresponds to the connected component of the graph obtained by disregarding the directionality.

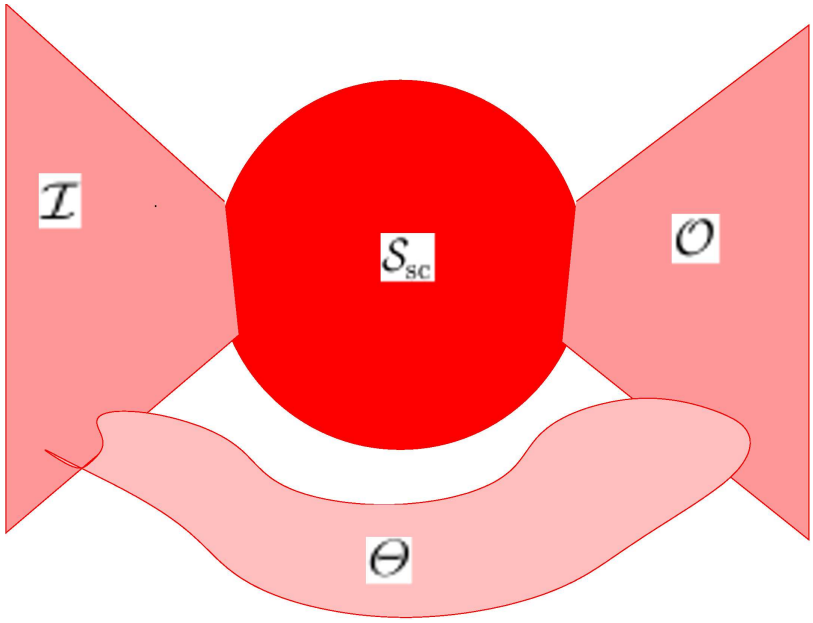

Fig. 13. A sketch of the bow-tie structure characteristic of a DRG's topology [Dorogovtsev *et al.*, 2001]: the two bows correspond to the giant components $\mathcal{I} \setminus \mathcal{S}_{\rm sc}$ and $\mathcal{O} \setminus \mathcal{S}_{\rm sc}$, respectively, whereas the tie represents the giant strongly connected component $\mathcal{S}_{\rm sc} = \mathcal{I} \cap \mathcal{O}$. Here we consider the most general case, in which $\mathcal{W} = \mathcal{I} \cup \mathcal{O} \cup \Theta$, where Θ contains in particular the paths linking the two bows without passing across the tie $\mathcal{S}_{\rm sc}$, as observed in some real networks such as the web [Broder *et al.*, 2000].

The analogue of the phase transition in the previously discused case of an undirected random graph may be characterized in a DRG by the formation of a giant in-component $\mathcal{I}$, containing $I = s_{\rm I} N$ nodes; of a giant out-component $\mathcal{O}$, containing $O = s_{\rm O} N$ nodes; of a giant strongly connected component $\mathcal{S}_{\rm sc} = \mathcal{I} \cap \mathcal{O}$, containing $S_{\rm sc} = s_{\rm sc} N$ nodes; and of a giant weakly connected component $\mathcal{W}$, containing $W = s_{\rm w} N$ nodes. In fact, one usually expects to observe two different transitions, *i.e.* two different abrupt changes in the properties of the system in the large-N limit: (i) at the lower average in/out-degree $z_{\rm c}^{\rm w}$, which corresponds to the critical average degree in the undirected graph, at which the giant weakly connected component $\mathcal{W}$ appears; and (ii) at the higher average in/out-degree $z_{\rm c}^{\rm d}$, at which the effective transition in the DRG occurs, namely at which the two giant components $\mathcal{I}$ and $\mathcal{O}$ appear simultaneously.

For $z \geq z_{\rm c}^{\rm d}$, the resulting bow-tie structure is sketched in [Fig. 13] and has been observed in many different real networks [Broder *et al.*, 2000; Ding *et al.*, 2009]. Notice that the appearance of the giant in-component $\mathcal{I}$ corresponds to the divergence of the number of nodes that can be reached from a given one, while that of the out-component $\mathcal{O}$ corresponds to the divergence of the number of nodes from which a given one can be reached; *i.e.*, a node is in the giant in-component if its out-component diverges, and vice-versa.

Moreover, above the transition, it may be necessary to introduce one more giant component in order to fully characterize the topology, since it is possible to have $(\mathcal{I} \cup \mathcal{O}) \subset \mathcal{W}$, while $\mathcal{W} \setminus (\mathcal{I} \cup \mathcal{O}) \neq \varnothing$. The latter is, in particular, the case when there are directed paths between $\mathcal{I}$ and $\mathcal{O}$ that do not pass across $\mathcal{S}_{\rm sc}$. Such a set $\Theta = \mathcal{W} \setminus (\mathcal{I} \cup \mathcal{O}) \neq \varnothing$ has been found in the structure of the web [Broder *et al.*, 2000] —

which can be seen as a DRG characterized by a power-law distribution in/out-degree — and is shown in [Fig. 13].

The generating-function formalism for DRGs [Newman *et al.*, 2001; Dorogovtsev *et al.*, 2001] turns out to be particularly simple when the in/out-degree distribution factorizes, $\mathcal{P}_{k_{\rm in},k_{\rm out}} = \mathcal{P}_{k_{\rm in}}\mathcal{P}_{k_{\rm out}}$, since the in- and out-components are independent in the large-N limit, so that one simply has $s_{\rm sc} = s_{\rm I}s_{\rm O}$. For the case of $\mathcal{P}(k_{\rm in}) = \mathcal{P}(k_{\rm out})$, with the Poisson distribution $\mathcal{P}(k)$ given by Eq. (30), the transition does still occur at the critical average in/out-degree $z_{\rm c}^{\rm d} = \langle k\rangle_{\rm c} = 1$, and the giant in- and out-components have the same size:

$$s_{\rm I} = s_{\rm O} = 1 - r, \tag{35}$$

where r is once more given by the solution of Eq. (34). Thus $s_{\rm sc} = (1-r)^2$, whereas the fraction of nodes in $\mathcal{I} \setminus \mathcal{S}_{\rm sc}$, and equivalently in $\mathcal{O} \setminus \mathcal{S}_{\rm sc}$, equals $r(1-r)$: the three regions in the bow tie have roughly the same size in the thermodynamic limit. This result has likewise been observed in real networks [Broder *et al.*, 2000], for $r \simeq 1/2$, and hence $z \simeq \log 4$. Moreover, one simply has $z_{\rm c}^{\rm w} = z_{\rm c}^{\rm d}/2$: when r is a solution of Eq. (34) one has $r(2z) = r^2$, and it follows that, for $z > z_{\rm c}^{\rm d}$, $s_{\rm w} = 1 - r^2 = s_{\rm I} + s_O - s_{\rm sc}$, which confirms that here $\mathcal{W} = \mathcal{I} \cup \mathcal{O}$ and $\Theta \approx \varnothing$.

An important implication from this analysis for the present damage-propagation study is that nodes lying outside the giant connected component $\mathcal{W}$ are "screened," *i.e.* protected from any perturbation starting inside the giant component.

Another key property of the topology of Erdős-Rényi random graphs is that their structure is tree-like for p-values that are not too large. This property holds rigorously for the finite-size connected components, both below and above the critical point, since it can be shown that the probability of closed loops occurring approaches zero in the limit $N \to \infty$; it is at least locally valid within the giant connected components, where their occurrence can be neglected in a first approximation.

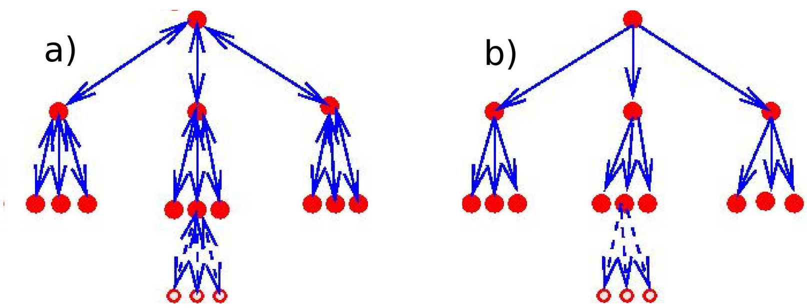

Fig. 14. The local tree-like structure characteristic of Erdős-Rényi random graphs: damage spreading (a) on an undirected random graph $G(N,p)$, with $\langle k\rangle = 3$; and (b) on a DRG $D(N,p)$, with the same mean degree $\langle k_{\rm out}\rangle = \langle k_{\rm in}\rangle = 3$.

We compare in [Fig. 14] these locally tree-like structures for a undirected random graph and a DRG with the same $z = 3$ value: notice that, in the first case, one has $z_2 = z^2$ from Eq. (32), while in the second case, one gets the same kind of result, with $z_2 = \langle k_{\rm in}\rangle\langle k_{\rm out}\rangle = z^2$. In other words, in DRGs, the probability $\mathcal{P}(\{i \to j\} \wedge \{j \to i\})$ to have both the link $i \to j$ and the link $j \to i$ present equals roughly p^2, and it is therefore negligible when $p \ll 1$, which is the case of typical interest here for large N. In undirected random graphs, though, one has — in order to make a meaningful computation — to also consider the edges that emerge from a given node, apart from the one along which the signal arrived.

As we shall see below, this difference is evident in the results for damage spreading over just a short time in BDE models on random graphs. These numerical results can be predicted quite accurately on the basis of the local tree-like topology. Moreover, when considering asynchronous updating due to randomly selected delays, two paths with the same space length still have, in general, unequal time lengths; but the locally tree-like topology implies that the number of distinct concurrent paths that connect two given nodes does not increase as fast with the average in/out-degree $\langle k_{\rm in}\rangle = \langle k_{\rm out}\rangle$ as in the deterministic braid chains of Section 3.

4.2. *Synchronous free model*

We start again with the simplest case, the one of the free models — defined by Eq. (3), with all the delays equal to the same time unit $\tau_0 = 1$ day, on the DRG $D(N,p)$ — and we study as usual the consequences of a natural disaster impairing the activity of a single firm for a duration τ_c. For simplicity, we limit the analysis to the case $\tau_c = \tau_0$.

For a DRG, the possibility exists of a link being selected with probability $p = 0$, *i.e.* of such a link being absent altogether from the geometric configuration Ω of the network. While the random selection still occurs only when setting up the BDE, it now involves not just the set of delays $\mathcal{T}$ but also Ω. For the sake of concision, we introduce the notation $\Omega^* = (\Omega, \mathcal{T})$ to refer to the random set-up involving both network geometry and BDE delays.

In the presence of randomness in the network selection, the BDE system (2) can no longer be reduced, as in Section 3.1, and one has in principle to solve a set of N equations in N variables; this set of BDEs can be rewritten in the form:

$$x_i(t) = \prod_{j \in \mathcal{I}(i)} x_j(t - \tau_0) \qquad i = 1, ..., N. \tag{36}$$

The Boolean product here runs over all the indices j labeling the firms that are suppliers of i. We denote this set of nodes by $\mathcal{I}(i) = \{j : A_{ij} \neq 0\}$; the in-degree $I(i)$ of node i is the total number of its suppliers *i.e.* $I(i) = k_{\text{in}}(i)$. Analogously, the out-component $\mathcal{O}(i) = \{j : A_{ji} \neq 0\}$ of node i corresponds to the firms that are its customers; their total number is $k_{\text{out}}(i)$.

It is clear from Eq. (36) that the properties of this DRG model strongly depend upon the probability distributions of the in- and out-degree. We assume $k_{\text{in}}(i)$ and $k_{\text{out}}(i)$ to be independent and given by Eq. (30), with mean values that satisfy $\langle k_{\text{in}}(i)\rangle = \langle k_{\text{out}}(i)\rangle = (N-1)p = z$. Hence, for increasing z values, the statistical properties of the solutions will reflect the appearance of giant connected components in the model's graph. In particular, one expects to find fundamentally different kinds of solutions for an average in/out-degree that is lower or higher than the critical value $z_c^d = \langle k \rangle_c = 1$.

The damage spreading in this simple free model can, in fact, be understood with the same argument used for evaluating the average size of the connected components in the graph: at $t = 1$, the signal propagates from node i, occupied by the initially damaged firm, to its closest neighbors, whose average number is $z_1 = z$; at $t = 2$, it reaches its next-closest neighbors, whose average number is $z_2 = z^2$, and so on. From Eq. (32) it follows that, at time t, the damage did reach on average z^t nodes; hence:

$$[\text{DRG}] \qquad \langle \theta(t; \Omega)\rangle \simeq z^t, \text{ for } t \ll \log N / \log z. \tag{37}$$

This implies that the average number of impaired firms increases with time only if $z = \langle k \rangle > \langle k \rangle_c = 1$, *i.e.* only if the graph is above its transition point.

This argument does make use of the DRG's local tree-like structure, since we are implicitly assuming that the probability of two nodes reached at a given time step being themselves connected by a different path, *i.e.* the probability of closed loops, can be neglected. In fact, the argument breaks down roughly at the time when the signal has propagated to the whole connected component to which the initial node i belongs. At that time and later, one can find two distinct situations:

- Either i lies in a connected component containing a small number of nodes, and thus $S_c = 0(1)$. One then expects that there are no loops, and hence the system can completely recover from the initial damage, *i.e.* $\langle \rho_\infty(\Omega)\rangle = 1$: a randomly chosen initial node i does belong, in the large-$N \to \infty$ limit, to a connected component with a finite number of nodes, almost surely for subcritical degree $z = \langle k \rangle < 1$ and with probability r for supercritical degree $z = \langle k \rangle > 1$.
- The graph is above the critical point, $\langle k \rangle > 1$, and i belongs to a giant connected component. Because of the presence of closed loops, a finite fraction of the firms will be impaired in the asymptotic solution, and the production network will never recover completely from the initial damage.

Such results can be explained by noticing that, in our DRG model, there are firms that have no customers in the network. For these firms that lie at an end of the production chain, being unable to produce does not have any consequences on the rest of the chain but only on household well-being. Since

$z = \langle k \rangle$ measures the average number of customers in the network, in the limit of a large total number N of firms, one observes the previously mentioned phase transition: for $\langle k \rangle < 1$, most of the firms are either themselves in this "end-of-the-chain" situation, or have just a few customer firms that are in this peculiar situation, and so on; thus the initial damage does not usually propagate. Conversely, as soon as $\langle k \rangle > 1$ a finite fraction of the firms have customers in the network, which have themselves other customers and so on.

To make this analysis more quantitative, one can say in the large-N limit that, in a free DRG above the transition point, in order for damage to reach a finite fraction of the network, the initially attained firm has to belong to the giant in-component, $i \in \mathcal{I}$: this occurs with probability $1 - r$. Moreover, in this asymptotic limit, one expects that all the firms in the giant out-component $\mathcal{O}$ will eventually be impaired, which means a fraction $s_{\rm O} = 1 - r$ of the entire network. Correspondingly, we find:

$$\langle \theta(t;\Omega) \rangle \simeq \begin{cases} z^t & \text{for } t \ll \langle T_0(\Omega) \rangle, \\ (1-r)^2 N & \text{for } t \gg \langle T_0(\Omega) \rangle,\ N \gg 1, \end{cases} \tag{38}$$

where the time that $\langle \theta(t;\Omega) \rangle$ takes before reaching the asymptotic constant average value is also quite short for large N values, since it is of order $\langle T_0(\Omega) \rangle \sim \log((1-r)N)/\log z$.

Interestingly, $(1-r)^2$ is also the fraction of nodes in the network's giant strongly connected component $\mathcal{S}_{\rm sc}$. Nevertheless, the two quantities do have a different meaning: when the initial node belongs to $\mathcal{I}$, the total number of eventually impaired firms is $(1-r)N = S_{\rm O}$, which is definitely larger than $S_{\rm sc}$ for small r-values. This point can be better understood by looking at the Erdős-Rényi undirected random graphs having the same average degree $z > 1$: here, the initially damaged firm i has to belong to the giant connected component $\mathcal{S}_{\rm gc}$, and the firms whose activity is finally impaired are the ones in $\mathcal{S}_{\rm gc}$ as well; hence we find again that $\langle \theta(t;\Omega) \rangle$ approaches $(1-r)^2 N$ at large times, although $S_{\rm sc} = 1 - r$.

To summarize, the average asymptotic density of fully active firms is given, in the undirected random graph as well as the DRG, by

$$\langle \rho_\infty(z,\Omega) \rangle = 1 - (1-r)^2 = 2r - r^2, \tag{39}$$

where we recall that r is the solution of Eq. (34).

An important difference between the behavior of the synchronous free models on both directed and undirected random graphs concerns the short-time dynamics: as shown in [Fig. 14], in the undirected case the signal propagates also back to the node from which it has arrived. To correctly describe the behavior of $\langle \theta(t;\Omega) \rangle$, Eq. (37) should therefore be replaced by:

$$\text{[URG]} \qquad \langle \theta(t;\Omega) \rangle = \sum_{l=0}^{[t/2]} z^{t-2l} \text{ for } t \ll \log N / \log z, \tag{40}$$

where $[y]$ denotes, as usual, the integer part of y, *i.e.,* the largest integer smaller than y.

Numerical results on the average total number of impaired firms $\langle \theta(t;\Omega) \rangle$ in the synchronous free model on random graphs are presented in [Fig. 15]. In [Fig 15a], we compare the short-time behavior of $\langle \theta(t,\Omega) \rangle$ between the DRG and an undirected random graph with the same average degree $z = \langle k \rangle = 1.5$. In this case, the transient that precedes the attainment of the asymptotically constant value is relatively long, and the difference is appreciable between the DRG case — described by Eq. (37), with $\langle \theta(t,\Omega) \rangle \simeq z^t$ — and the undirected one, where the numerical results are in better agreement with $\langle \theta(t;\Omega) \rangle \simeq z^t + z^{t-2}$, which is an approximation of the sum on the right-hand side of Eq. (40). Notice, moreover, that the asymptotic values in both of the cases are nearly equal, as expected.

In [Fig. 15b], we plot the same quantity — computed for DRGs with different values of $z = \langle k \rangle > 1$ — and compare the numerically obtained curves with the expected short-time behavior given by z^t. It is clear from this figure that the asymptotic total number of impaired firms is an increasing function of the average in/out-degree. Moreover, already for z as small as $z = 5$, this number practically coincides with the system size N, thus implying that the damage spreads in just a few steps to all the firms, since $\langle T_0(\Omega) \rangle \simeq \log N / \log z$.

Our results on the average asymptotic density $\langle \rho_\infty(z,\Omega) \rangle$, as a function of the average in/out-degree $z = \langle k \rangle$, are presented in [Fig. 16]: they turn out to be in very good agreement with the expected curve,

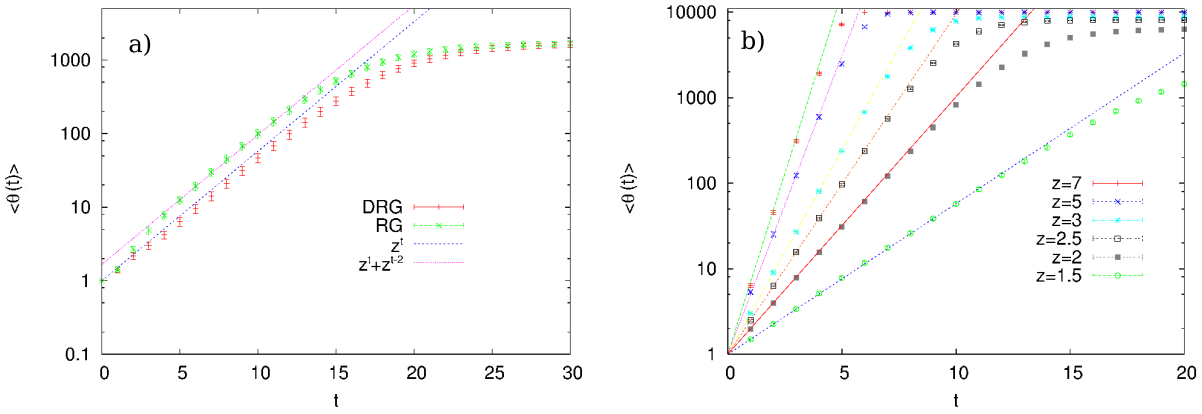

Fig. 15. Short-time behavior of the average total number of impaired firms $\langle\theta(t;\Omega)\rangle$ for synchronous free BDE models on random graphs, with a large number of nodes $N \gg 1$; the results are averaged over at least $\mathcal{N}_s = 200$ different configurations Ω of the links. (a) Comparison of $\langle\theta(t;\Omega)\rangle$, between the DRG $D(N,p)$, with average in/out-degree $z = \langle k\rangle = 1.5$, and the undirected Erdős-Rényi random graph $G(N,p)$, with the same $\langle k\rangle$ value; here $N = 5\ 000$. (b) Comparison between the behavior of $\langle\theta(t;\Omega)\rangle$ in the DRG $D(N,p)$, for different values of $z = \langle k\rangle$ above the transition point $z_c = 1$; here $N = 10\ 000$. The numerical results are also compared with the corresponding expected behavior, given by Eq. (37) for DRGs, and by an approximation of Eq. (40) for undirected random graphs, respectively. See text for details.

cf. Eq.(39), obtained by evaluating numerically the solution r of Eq. (34). The numerical results in the figure are for DRGs, but we checked that in undirected graphs with the same average degree one gets definitely comparable results (not shown). This agreement also implies that for the number of nodes used here, $N = 10\ 000$, the corrections to the behavior of $\langle\rho_\infty(z,\Omega)\rangle$ in the limit $N \to \infty$ are already negligible.

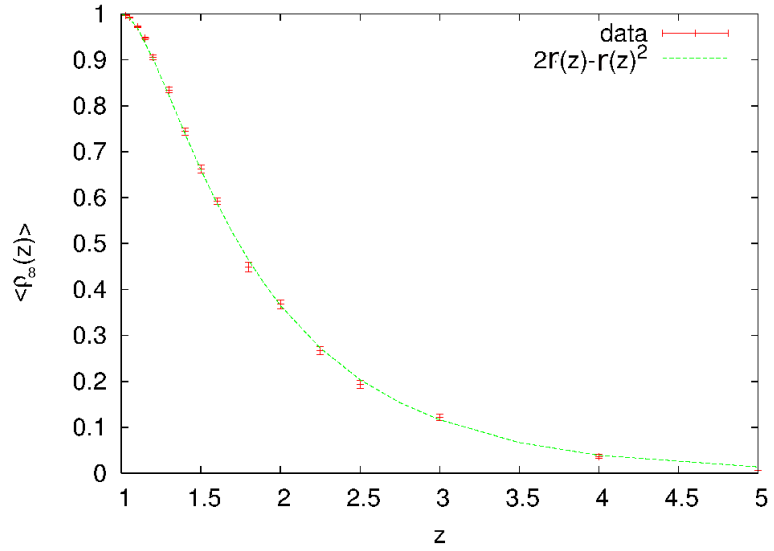

Fig. 16. Average asymptotic density $\langle\rho_\infty(z,\Omega)\rangle$ for synchronous free BDE models on DRGs with large network size, $N = 10000$; the results are averaged over at least $\mathcal{N}_s = 200$ different configurations Ω of the links. The asymptotic average density is plotted as a function of the average in/out-degree $z = \langle k\rangle$, and it is compared with the expected behavior, given by Eq. (39).

To conclude this section, we note that the study of these simple synchronous free models on random structures — which are more complex than those in Section 3 — might prove useful also for a better understanding of the topology of the networks themselves. The size of their connected components, in particular, is difficult to compute analytically in the case of realistic directed networks, in which the

probability distributions of the in- and out-degree do not factorize [Newman, 2007]. A first step in this direction would be to consider directed "small-world" networks [Watts, 1999]; such networks interpolate, in some sense, between the topology of a braid chain and that of an Erdős-Rény random graph.

4.3. *Asynchronous free model*

We now turn to the study of the free model on a DRG with random delays that are uniformly distributed in the interval $[\tau_{\mathrm{min}}, \tau_{\mathrm{max}}]$. The model is described by a set of BDEs analogous to Eq. (36):

$$x_i(t) = \prod_{j \in \mathcal{I}(i)} x_j(t - \tau_{ij}), \qquad i = 1, ..., N, \tag{41}$$

where $\mathcal{T} = \{\tau_{ij}\}$ is a set of quenched random variables, independently and uniformly distributed in the interval $[\tau_{\mathrm{min}}, \tau_{\mathrm{max}}]$. The time is in units of $\tau_{\mathrm{min}} = 1$ day, and we take as usual $\tau_{\mathrm{max}} = 10$ days, limiting moreover the analysis to the case in which the duration of the initial perturbation is $\tau_{\mathrm{c}} = \tau_{\mathrm{min}}$.

We start by noting that, in the first time step, the signal propagates on average to z/τ_{max} other firms. In the next time steps, one still expects — for networks above the transition point $z_{\mathrm{c}}^{\mathrm{d}} = \langle k \rangle_{\mathrm{c}} = 1$ — to observe an exponential spreading of the damage. Since the network topology is locally tree-like, the signal propagates, as in the previous subsection, independently along each given branch of the tree, and on to further and smaller branches. Since the propagation paths of different time lengths are not concurrent, the random delays are likely to show up first of all in a global rescaling of the time by a factor $1/\tau_{\mathrm{av}}$, where $\tau_{\mathrm{av}} = \langle \tau_{ij} \rangle$.

The average total number of impaired firms $\langle \theta(t; \Omega^*) \rangle$ is thus given by

$$\langle \theta(t; \Omega^*) \rangle = \frac{z}{\tau_{\mathrm{max}}} z_{\mathrm{eff}}^{t/\tau_{\mathrm{av}}} \text{ for } t \ll \log N / \log z_{\mathrm{eff}}; \tag{42}$$

note that now both the geometry Ω and the set of delays $\mathcal{T}$ are randomly selected, so we refer henceforth to the generalized configuration $\Omega^* = (\Omega, \mathcal{T})$. The effective average in/out-degree which appears in Eq. (42) has to approach z when $z \to 1^+$; hence $z_{\mathrm{eff}} \geq z_{\mathrm{eff}}^- = z$. To see this, note that Eq. (42) has to reduce to the synchronous case when all the delays equal $\tau_0 = 1$, whereas the presence of longer delays cannot but increase z_{eff}.

In fact, since the signal from a given node propagates to its customers up to the time $t + \tau_{\mathrm{max}}$, one finds an effective increase of the average in/out-degree, which can be easily bounded from above, as follows:

$$z_{\mathrm{eff}} \leq z_{\mathrm{eff}}^+ = z \sum_{l=0}^{\infty} \left(\frac{z}{\tau_{\mathrm{max}}} \right)^l = \frac{z}{1 - z/\tau_{\mathrm{max}}}. \tag{43}$$

Summarizing, for short times and for $z > 1$, we get:

$$f^-(t; z) \equiv f(t; z_{\mathrm{eff}}^-) \leq \langle \theta(t; \Omega^*) \rangle \leq f(t; z_{\mathrm{eff}}^+) \equiv f^+(t; z), \tag{44}$$

where

$$f(t; z_{\mathrm{eff}}) = \frac{z}{\tau_{\mathrm{max}}} z_{\mathrm{eff}}^{t/\tau_{\mathrm{av}}}. \tag{45}$$

The numerical results on $\langle \theta(t; \Omega^*) \rangle$ — obtained for several supercritical values $z > 1$ of the average in/out-degree — are compared in [Fig. 17] with the expected upper and lower bounds $f^-(z, t)$ and $f^+(z, t)$ on the short-time behavior, given by Eqs. (44) and (45). The computed curves always lie between $f^-(t; z)$ and $f^+(t; z)$, within a wide time window; they approach $f^-(t; z)$ for $z \to 1^+$, and $f^+(t; z)$ for large $z \gg 1$; in fact, the numerical results at short times nearly coincide with $f^+(t; z)$ already for z as small as $z = 3$.

In the large-time limit, since there are loops in the giant strongly connected component $\mathcal{S}_{\mathrm{gc}}$, one expects that the damage will spread to the whole giant out-component $\mathcal{O}$, with the same probability $1 - r$ as in the synchronous model with equal delays. We verified numerically that one still observes, for large N values, an asymptotic average density of fully active firms $\langle \rho_\infty(\Omega^*) \rangle = 2r - r^2$, in agreement with Eq. (39). Moreover, for N-values that are not too small, one usually gets the same asymptotic density $\rho_\infty(\Omega)$ for a given network configuration Ω, whether the delays are all equal or are randomly chosen, *i.e.* both in the synchronous and

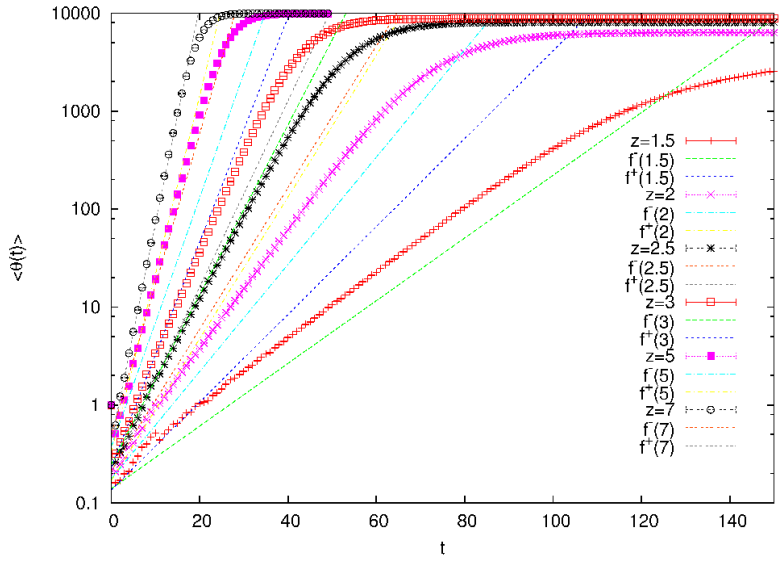

Fig. 17. The average total number of impaired firms, $\langle \theta(t, \Omega^*) \rangle$, as a function of time, in the free BDE model on a DRG, for different mean-degree values $z = \langle k \rangle$; the network size is $N = 10\,000$. The results are averaged over at least $\mathcal{N}_s = 200$ different configurations of the links Ω and of the random delays $\mathcal{T}$, and $\Omega^* = (\Omega, \mathcal{T})$. The numerical results for each z-value are compared with the expected short-time lower and upper bounds, $f^-(t; z) = f(t; z^-_{\rm eff})$ and $f^+(t; z) = f(t; z^+_{\rm eff})$, respectively, where f is given by Eq. (45). See text for details.

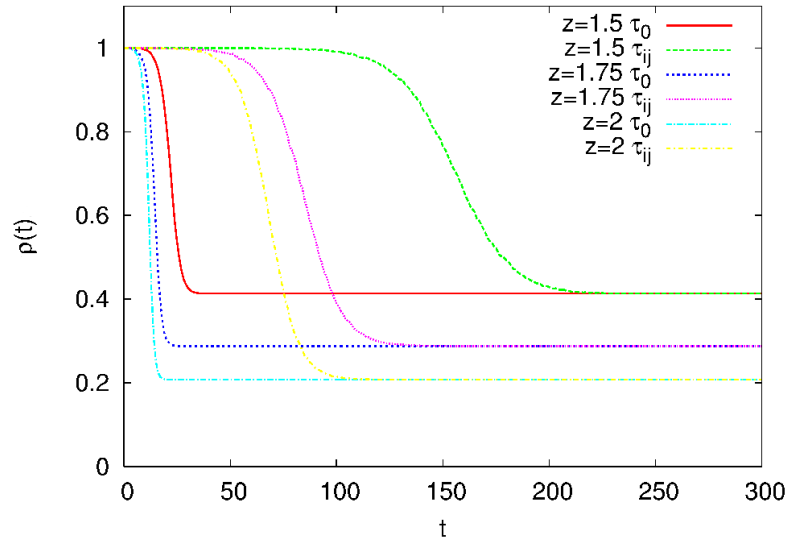

Fig. 18. The density of fully active firms $\rho(t, \Omega^*)$ as a function of time, for the free model on a DRG with three distinct, supercritical average connectivities, $z = 2.0, 1.75$ and $1.5 > 1$. Here we consider a single typical configuration Ω of the links, and compare the results for delays taken all equal to $\tau_0 = 1$ day with those for a single typical configuration $\mathcal{T}$ of randomly selected delays, chosen to be uniformly distributed between $\tau_{\rm min} = 1$ day and $\tau_{\rm max} = 10$ days. Note that the densities approach exactly the same asymptotic value in both cases, and for all four z-values considered.

in the asynchronous model. This can be qualitatively understood because, if the initially impaired firm is in a connected component in which there are no loops, the economy can recover completely in both cases, whereas if it is in the giant in-component then the damage spreads to the whole out-component of the network.

Nevertheless, the asymptotic solutions for the free BDE systems on the same DRG configuration Ω

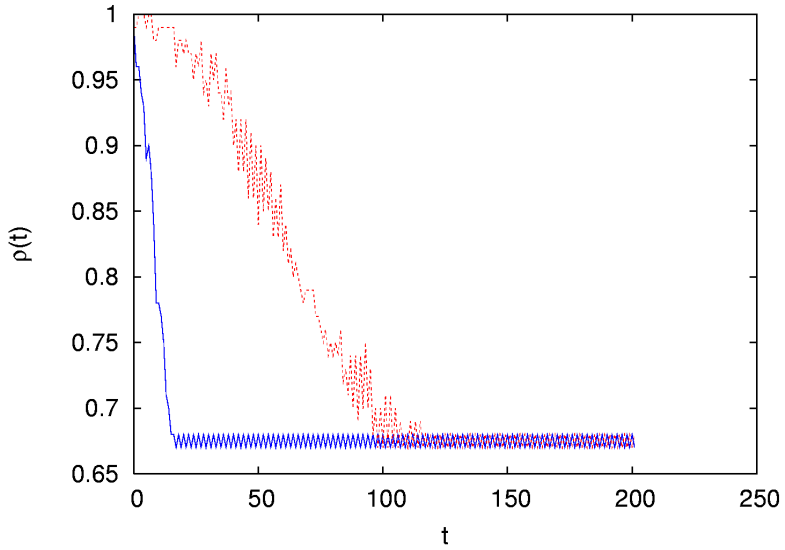

Fig. 19. The density of fully active firms $\rho(t;\Omega^*)$ as a function of time, in a given DRG configuration Ω with $z = \langle k\rangle = 0.525$ and $N = 100$. We compare results for synchronous updating, with all delays equal to $\tau_0 = 1$ day (lower, blue curve), to the ones for a single typical configuration of random delays $\mathcal{T}$, uniformly distributed between $\tau_{\min} = 1$ day and $\tau_{\max} = 10$ day (upper, red curve). Notice that the transient is much longer for the asynchronous updating, but the asymptotic solutions display the same behavior of the density, which is periodic with a mean value definitely smaller than one, although the network is quite subcritical, with $z < \langle k\rangle_c = 1$. See text for details.

do not need to coincide in the synchronous and asynchronous case. This effect occurs for relatively small N, near or below the critical point, $z = \langle k\rangle \lesssim 1$, since it is related to the presence of loops in connected components that contain a large enough fraction of the nodes, but are not the giant ones.

While a detailed analysis of the finite-N behavior of free BDE models on DRGs is beyond the scope of the present paper, we show in [Fig. 19] and in [Figs. 20a–i] examples of time-variable asymptotic behavior, for DRG configurations Ω with $N = 100$ and with $z = 0.525$, *i.e.* well below the critical point. We note that the observed behavior may also depend upon the position i^* of the firm that is initially damaged, which is taken here to be $i^* = 1$ in all the computations. Nevertheless, our results are qualitatively the same for other choice of i^* (not shown).

We note first that, when the economy does recover completely, then it does so in the asynchronous as well as in the synchronous model; it is only when there is no complete recovery that one observes differences between the two. We compare in [Fig. 19] the numerical results on the density $\rho(t,\Omega^*)$ of fully active firms for the synchronous-updating case of all delays equal to $\tau_0 = 1$ day with those for a typical configuration of randomly selected delays, uniformly distributed between $\tau_{\min} = 1$ day and $\tau_{\max} = 10$ days; the duration of the initial damage is $\tau_c = 1$ day in both these cases.

The transient for the asynchronous updating (red curve) is much longer than for the synchronous one (blue curve), but the asymptotic solutions display the same type of behavior, with small-amplitude, distinctly periodic oscillations around a mean value of $\rho_\infty^{\varpi} \simeq 0.67 < 1$, although the network lies well below the critical point $\langle k\rangle_c = 1$.

The results in the nine panels of [Fig. 20] confirm that the differences between asynchronous and synchronous updating, for the same randomly selected network configuaration Ω, can be quite substantial:

- The transients are never shorter, and typically quite a bit longer, for asynchronous updating, cf. panels (c) and (g) here, as well as [Fig. 18] and [Fig. 19]; often, though, they can be of a length that is comparable to the case of synchronous updating.
- The asymptotic mean density is always higher for asynchronous updating, and sometimes the difference is appreciable; see again panels (c) and (g).
- The asymptotic behavior for the synchronous-updating case involves not only constant and periodic den-

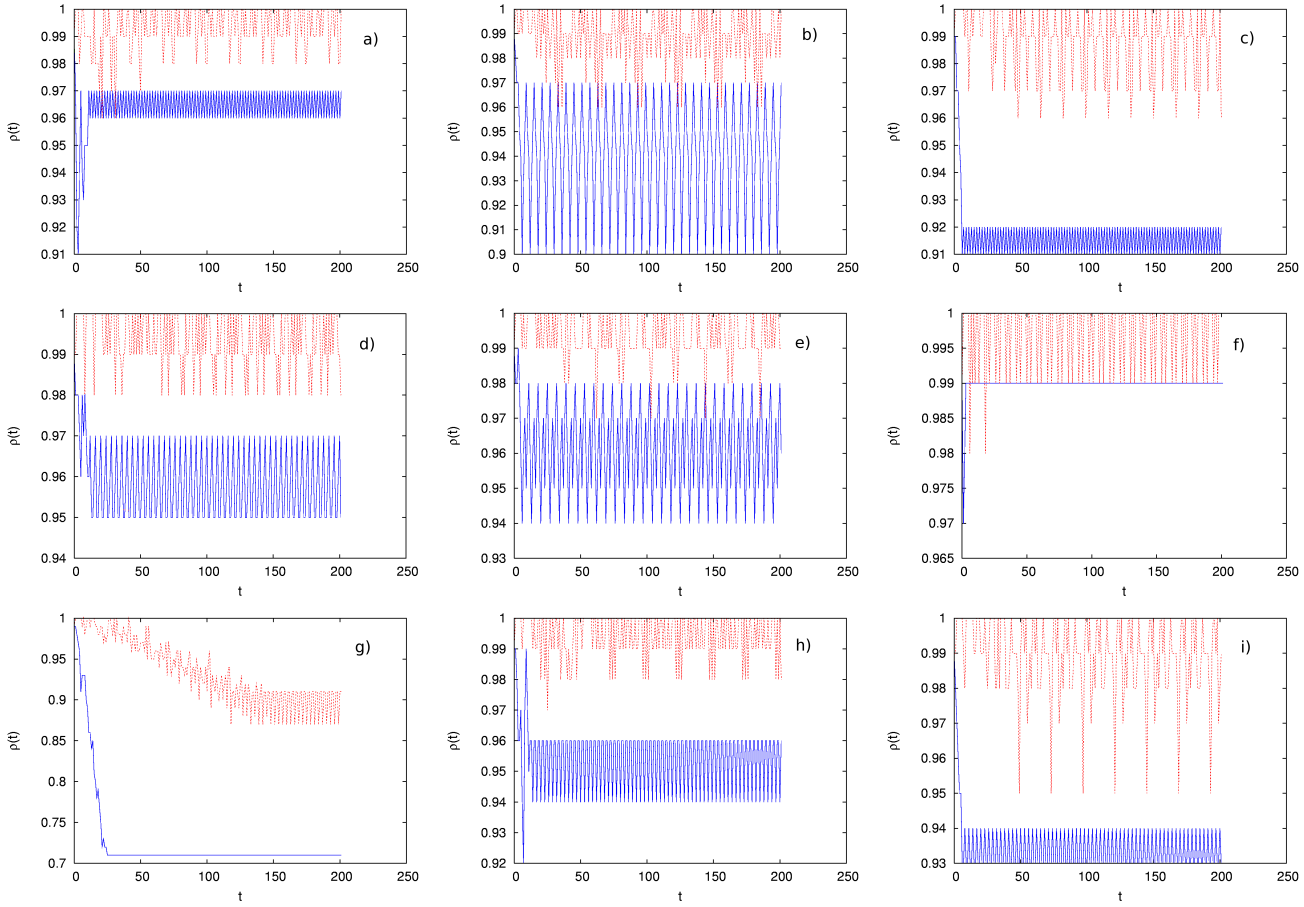

Fig. 20. The density of fully active firms $\rho(t;\Omega^*)$ as a function of time, for nine random network configurations Ω^*, all with $z = 0.525 < 1$. In all nine cases, we compare results for synchronous (blue curves) with those for asynchronous updating (red curves) on the same network geometry Ω; the latter results are for single, typical configurations $\mathcal{T}$ of randomly selected unequal delays. Notice that here the densities approach definitely distinct types of asymptotic behavior in the two cases. See text for details.

sities, but also doubly-periodic solutions, as in panel (e).

- The asymptotic behavior for the asynchronous-updating case appears to be always more complex than in the synchronous case — doubly periodic vs. constant, as in panel (f), or aperiodic vs. constant or purely periodic, as in panels (g) and (i).
- The amplitude of the oscillations when the updating is asynchronous is typically larger than when it is synchronous, cf. panels (a, c, f, g, i), but it can also be comparable, cf. panels (d, h) or even substantially smaller, cf. panels (b, e).

The probability of such complex behavior is not negligible, since we have observed the same kind of results in roughly (1/10)th of the configurations $\Omega^* = (\Omega, \mathcal{T})$ we studied.

4.4. *Forced DRG models*

We conclude this work by presenting some preliminary results on synchronous and asynchronous updating for forced models — as defined by Eqs. (1), (2) and (4) — on a DRG.

The equation for each x_i of system (2) can be written as:

$$x_i(t) = \overline{x}_i(t-\tau_0) \vee \left[\prod_{j \in \mathcal{I}(i)} x_j(t-\tau_0) \right] \tag{46}$$

for synchronous updating, with all delays equal to $\tau_0 = 1$ day, and:

$$x_i(t) = \prod_{j \in \mathcal{I}(i)} \left[\overline{x}_i(t - \tau_{ij}) \vee x_j(t - \tau_{ij})\right] \tag{47}$$

for asynchronous updating, with randomly selected delays $\mathcal{T} = \{\tau_{ij}\}$. We study, as usual, the propagation of the perturbation after initial damage to a single firm, which we take for simplicity of duration $\tau_c = 1$ day.

We start by noting that, when the economy recovers completely in the free models considered in Sections 4.2 and 4.3, it recovers completely also in the present forced models; hence the asymptotic solution is $x_i \equiv 1$. This happens when the initially damaged firm belongs to a component that contains no loops. For large N, this is the case almost surely below the DRG's critical point, $\langle k \rangle_c = 1$, and with probability r for $z = \langle k \rangle > 1$, where r is the fraction of nodes disconnected from the giant connected component $\mathcal{S}_{gc}$ and is given by the solution of Eq. (34).

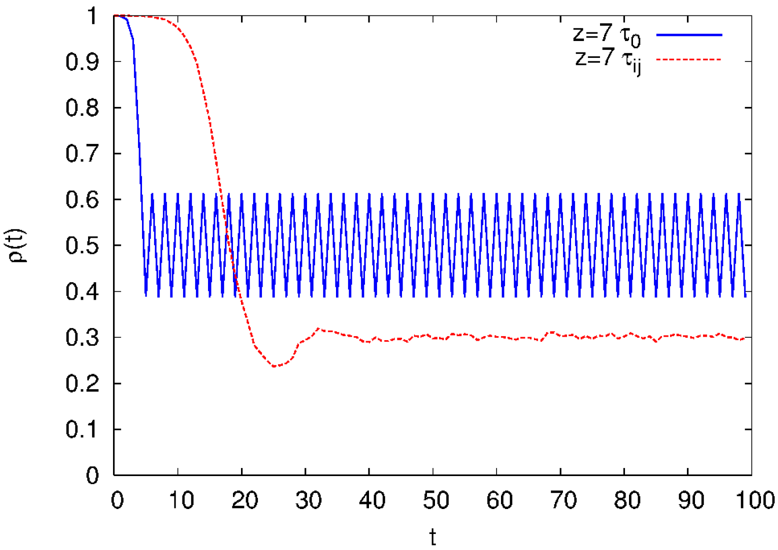

Fig. 21. The density of fully active firms $\rho(t;\Omega^*)$ as a function of time, in the forced model on a DRG with a large network size $N = 10\ 000$ and average input/output degree $z = 7 \gg \langle k \rangle_c$. Here we compare the results for synchronous (blue curve) vs. asynchronous updating (red curve), as in [Fig. 19].

When there are no loops, the locally tree-like argument provides a fully adequate explanation of the dynamics in the free models, but the production does recover completely at the end; likewise, at least partial recovery occurs when there are only a few loops present in the network. The fact that the asymptotic density is usually zero for z large enough in the free models is due to the presence of a large number of loops. Nevertheless, because of the external rescue inputs that we consider in the present subsection, one expects that, even for high supercriticality $z \gg 1$, though the damage spreads almost surely ($r \ll 1$) to the whole giant connected out-component, $\mathcal{O}$ — whose size is approximately N in this limit — the average fraction of healthy firms in the asymptotic solution is larger then zero, *i.e.* the economy can recover, at least partially.

In fact, for synchronous updating, since each firm recovers either if all of its suppliers did recover or if its activity has been already impaired for a duration τ_0, one expects that the average firm is fully active one half of the time. More precisely, $\langle \rho_\infty(z, \Omega^*) \rangle = 1 - (1 - r)^2/2 \simeq 1/2$, for $z \gg 1$. In the presence of randomly selected delays — since there is a larger number of concurrent paths of different lengths, and the activity of a given firm can be impaired for a duration that depends upon the good which is lacking — the asymptotic average density is expected to be smaller.

Our numerical results on the evolution of of $\rho(t;\Omega^*)$ — for a single, typical DRG configuration, with $N = 10\ 000$, and average in/out-degree $z = 7 \gg \langle k \rangle_c = 1$ — are given in [Fig. 21]. For synchronous

updating (blue curve), the asymptotic density is periodic with mean value $\rho_\infty \simeq 0.5$ and a peak-to-peak amplitude of 0.2, whereas for asynchronous updating (red curve), it fluctuates slightly around the lower value $\rho_\infty(\Omega^*) \simeq 0.3$. Notice that in the free models on the DRG one has, cf. [Fig. 16] in Section 4.2, $\langle\rho_\infty(\Omega^*)\rangle \simeq 0$ for $z = \langle k\rangle \gtrsim 5$; hence the external rescue inputs do allow a partial recovery of the activity, as expected. Moreover, in the asynchronous-updating case, the amplitude of the fluctuations is much smaller (by a factor of 10 or more) than in the synchronous case, where about $0.2N \simeq 2000$ firms are involved in this oscillating behavior between being fully active and impaired.

A qualitative explanation of the results in [Fig. 21] starts by arguing that the damage is initiated on the periphery of the DRG's connected component and spreads rapidly towards the center. Then, because of the external inputs, most of the economic network recovers, apart from a few firms that are once again on the periphery, and have been reached later by the wave of damage: these firms will be responsible for the next negative impulse. Roughly speaking, the nodes with larger in/out-degree are the ones that occupy the most central positions in the DRG, whereas having a small in-degree means that a node is less likely to be reached by the damage propagation, and a small out-degree means that it is less likely to transmit the damage; whether it is their in- or the out-degree that is small, these nodes lie on the network's periphery.

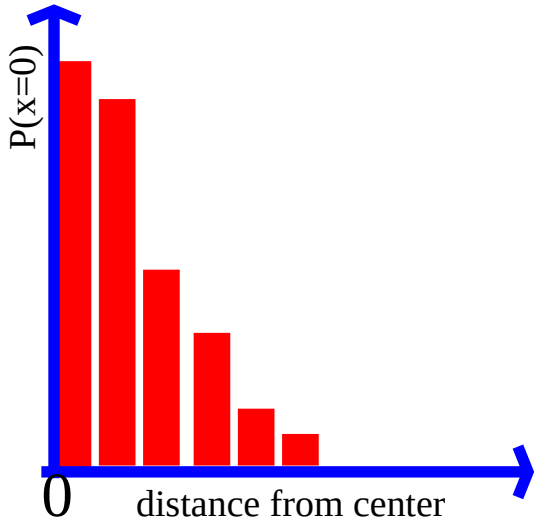

Fig. 22. A qualitative sketch of the expected fraction of impaired firms as a function of the distance of their position from the center of the connected component of the graph. See text for details.

The picture resulting from these considerations is sketched in [Fig. 22]; it implies that the degree of connectedness of a firm does have important implications for its staying free of damage. The results in [Fig. 21], in turn, speak to the important role of waiting times in a production chain for the up- and down-time of firms: the fact that these times are not all equal can actually smooth out fluctuations in the health of a large fraction of the firms in such a chain.

5. Concluding remarks

5.1. *Summary*

We have studied the propagation through various kinds of networks of initial damage at a single node. Our motivation was damage propagation through production networks, but the results are fairly general. The initial damage here was assumed to affect a single firm for a given time τ_c. Boolean delay equations (BDEs) were used to model the dynamics on the network, and we distinguished between *free models*, which represent closed, isolated networks, and *forced models*, in which external resources can help mend the damage. We also considered two kinds of network topologies, namely periodic braid chains (Section 3) and directed random graphs (DRGs; Section 4), as well as two types of distributions of delays, associated

with synchronous and asynchronous signal propagation, respectively.

The results of the entire investigation are summarized in [Tab. 3] and we highlight the most important ones herein. In the free models, the local-firm dynamics is controlled by a logical AND function of the inputs, and the damage can invade a finite fraction of the nodes or even the whole network when the following two conditions are fulfilled: (i) the mean input connectivity of the nodes is larger than unity; and (ii) the duration τ_c of the initial damage is larger than or equal to the smallest propagation time between two nodes. Such is the case for a braid-chain topology: ultimately — in the absence of external inputs — the production of all the firms is impaired.

Damage spreading velocity depends sensitively upon network topology: we have shown that the number $\theta(t)$ of impaired firms increases linearly with time for the braid chain and exponentially for the DRGs. When the network updating is asynchronous and the delays $\mathcal{T} = \{\tau_{ij}\}$ are randomly selected, $\tau_{\min} \leq \tau_{ij} \leq \tau_{\max}$, we have found that the propagation velocity is dominated by the fastest segments in the braid chain, *i.e.* by the shortest delay, while it is the average delay that limits propagation speed on the DRG. Moreover, in the random networks — and in the absence of external inputs — the saturation level of the fraction of impaired firms depends only upon the particular network topology, through the size of the connected component, which becomes necessarily non-empty as soon as the mean in/out-degree is larger than one.

In the forced models, external supplies do limit the damage, and periodic waves of damage move across the braid chains with equal delays, $\tau_{ij} = \tau_0 = 1$. For the DRGs with randomly selected $\mathcal{T}$, the asymptotic solutions are, of course, not exactly periodic but *cyclostationary* [Gardner *et al.*, 2006], and the duration of the transient before this behavior is reached diverges exponentially with network size N; still, the average density of fully active firms approaches a nearly constant value after a definitely shorter effective transient. This effective transient corresponds approximately to the duration of the first cycle of propagation of the damage across the connected component of the network; the latter “first transit” occurs, like in the free models, with linear or exponential speed, depending on the topology. Finally, periodic dynamics also prevails when the duration of the initial damage τ_c is smaller than the smallest propagation time $\tau_{\min}$ between two nearest-neighbor nodes.

Table 4. Overview of the main results obtained in the present work; each box in the table indicates the results in the model defined by the column with respect to the behavior of the quantity indicated in the row. As in [Tab. 2] of Section 2, we label by **Free** the free models governed by Eq. (3) and by **Forced** the forced models obeying Eq. (4); the synchronous case of all delays equal to τ_0 is labeled **Sync** and the asynchronous random-delay case, is labeled **Async**; **Chain** refers to the braid chain network in [Fig. 1], and **DRG** to the directed random graph, with the link probability $\mathcal{P}(A_{ij})$ given by Eq. (1). We summarize the results — depending upon the network's (average) in/out-degree k — with respect to the nature of the decay in time of the density $\rho(t)$ of fully active nodes, the effective transient time T_0, the asymptotic density ρ_∞, the transient time T_ϖ for reaching periodic behavior, and the period ϖ of the asymptotic solution; r is the fraction of nodes that do not belong to the giant connected component $\mathcal{S}_{\rm gc}$. All the results in this table refer to the case in which the duration of the initial perturbation is equal to the shortest delay in the model.

Chain, $k=1$	Free, Sync	Forced, Sync	Free, Async	Forced, Async
ρ-decay	const.	const.	const.	const.
T_0	0	0	0	0
ρ_∞	1-1/N	1-1/N	1-0.182/N	1-0.182/N
T_ϖ	0	0	0	0
ϖ	N	N	$N(\tau_{\max}+1)/2$	$N(\tau_{\max}+1)/2$
Chain, $k\geq 2$	Free, Sync	Forced, Sync	Free, Async	Forced, Async
ρ-decay	linear in t	linear in t	linear in t	linear in t
T_0	$(N-1)/(k-1)$	0	$\lesssim N/[k-(\tau_{\max}-1)]$	$\lesssim N/[k-(\tau_{\max}-1)]$
ρ_∞	0	$1-k/N$	0	$0<\rho_\infty<1$
T_ϖ	$(N-1)/(k-1)$	0	$\lesssim N/[k-(\tau_{\max}-1)]$	$\sim e^{{\rm const}N}$
ϖ	0	N/k	0	$\sim e^{{\rm const}N}$
DRG, $\langle k\rangle\geq 2$	Free, Sync	Forced, Sync	Free, Async	Forced, Async
ρ-decay	exponential in t	exponential in t	exponential in $2t/(\tau_{\max}+1)$	exponential in $2t/(\tau_{\max}+1)$
T_0	$\sim \log[(1-r)N]/\log z$	$<\log N/\log z$	$<\tau_{\max}\log N/\log z$	$<\tau_{\max}\log N/\log z$
ρ_∞ $(N\gg 1)$	$2r-r^2$	~ 0.5 $(z\gg 1)$	$2r-r^2$	$0<\rho_\infty<0.5$ $(z\gg 1)$

The models that we have used are highly simplified with respect to real production networks, and the behavior of firms has been represented in a highly idealized way. Still, results from this simple analysis suggest that:

- Even very localized damage does spread in the absence of sufficient stocks and flexibility; as a result, production shortages will last and can persist for times that are much longer than the duration of the initial local damage. This result suggests that an economy can suffer from disaster consequences even after all physical damages have been repaired.
- The presence of multiple concurrent production and trading paths with different delivery times does not necessarily imply a slowing down of the speed of the signal, which can propagate as fast as the shortest path, depending on the network topology. This result suggests that it is the most vulnerable supply chains that control the macroeconomic losses and that vulnerability analysis should focus on the identification of key weaknesses in production and trading patterns.

Finally, the very simplicity of the models studied herein — while limiting their direct usefulness in concrete situations — also suggests many areas of application that differ from our initial, production-chain motivation. We turn now to a brief overview of some of these areas, emphasizing in particular the ones that might be associated with climatic applications.

5.2. *Applications to the geosciences*

We have already mentioned in Section 1.2 some of the other areas in which the present approach to local damage propagation across a network might be of interest. They include, in the socio-economic domain, logistics [Bak *et al.*, 1993], infrastructures [Haimes & Jiang, 2001], and finance [Delli Gatti *et al.*, 2005; Battiston *et al.*, 2007], while in the geosciences they include earthquake dynamics [Zaliapin *et al.*, 2003a,b; Ghil *et al.*, 2008], forest fires [Spyratos *et al.*, 2007] and river networks [Zaliapin *et al.*, 2010], as well as climatic variability [Tsonis & Swanson, 2008; Donges *et al.*, 2009]. Finally, life-science applications include food webs [Carpenter *et al.*, 1985] and immunology [Kaufman *et al.*, 1985; Neumann & Weisbuch, 1992; Perelson & Weisbuch, 1997], among many others.

We discuss now very succintly the network modeling of climatic variability, following [Tsonis & Swanson, 2008; Donges *et al.*, 2009]. The idea that meteorological, oceanographic or coupled climatic variability might involve "centers of action" that are widely separated in space goes back to H. H. Hildebrandsson and L. P. Teisserenc de Bort [Hildebrandsson & Teisserenc, 1907] and to G. Walker's "teleconnections" between them [Walker & Bliss, 1932]. The statistical and dynamical study of such teleconnections engaged many important figures in the history of these disciplines over the last century [Bjerknes, 1969; Hoskins & Karoly, 1981; Wallace & Gutzler, 1981]. The closest in spirit to the approach presented here might be found in [Ghil & Mo, 1991, Fig. 14]; see [Saunders & Ghil, 2001] for a BDE treatment of the El-Niño/Southern-Oscillation (ENSO) mechanism postulated by J. Bjerknes in [Bjerknes, 1969].

Many of the dynamical studies of the atmosphere's low-frequency variability that involve teleconnections have used the highly simplified geometry of a so-called β-channel with periodicity in longitude and solid walls along parallels to the north and south of the channel, away from both the North Pole and the Equator [Ghil & Childress, 1987; Pedlosky, 1987; Chen *et al.*, 2003]. We saw in the present paper that signal propagation on a braid chain can be quite different from that in a more random configuration in the plane or, possibly, on the sphere [Hoskins & Karoly, 1981]. Thus BDE models in such geometrically different settings might provide some guidance to network-based investigations of teleconnections and climate variability.

Efforts are currently under way to expand further the applications of the approach presented here to the geosciences. In [Zaliapin *et al.*, 2010], the authors introduced a dynamic-tree framework for the study of *envirodynamics* on river networks, and suggested modeling the transport along real and synthetic networks by using BDEs. The dynamic tree of a river basin does take into account the differing flow times along the edge of the conventional, static tree. Both the dynamic and the static tree can be well approximated by self-similar Tokunaga trees (also called Tokunaga SSTs), but the two types of trees have different self-similarity parameters. BDEs can provide easy-to-explore, preliminary models of the actual flow of water

through the edges, as well as of the flow of sediment, biomass, and pollutants. The downstream effects of chemicals being released at a node, for instance, could be modeled along the lines presented here. We expect such models to shed further light on the complex and important problems of transport on river networks.

In [Zaliapin *et al.*, 2003a,b], a BDE model of *colliding cascades* on a ternary tree that represents a network of successively smaller scales in Earth's crust was studied. Seismic load cascades down from the largest scales or "plates" to the smallest, while failures cascade up from the smallest to the largest plates. It would clearly be of interest to study failure propagation on more complex fault networks of DRG type. Similar generalizations could be formulated for the heterogeneous models of forest fires introduced in [Spyratos *et al.*, 2007].

Acknowledgements
It is a pleasure to thank the organizers of the two-day conference honoring the contributions of Catherine Rouvas-Nicolis ("Katy" for her friends) to applying the concepts and tools of complex systems in the field of weather and climate dynamics, as well as all the participants, for the success of this event. Conversations with Katy, no less than her papers, have provided stimulation to the field in general, and to many of us in particular. Constructive comments on the present paper by G. Nicolis and S. Vannitsem are appreciated. Work on this paper was initiated during the European Union's project "Extreme events: Causes and consequences (E2C2)." This project was coordinated by one of us (M.G.) and it brought together the authors of this paper with Katy and with many others. More recent support was provided to M.G. by NSF Grants DMS-0934426 and DMS-1049253.

Appendix A Braid chain with $k = 1$

In this appendix, we evaluate the average total number of impaired firms $\langle\theta(t;\mathcal{T})\rangle$ in the free model on a braid chain with $k = 1$. This number can be expressed, by using Eqs. (9) and (11), as a function of the probability $\mathcal{P}(T_n, n)$, where T_n is the sum of n random variables τ_{ij}:

$$\langle\theta(t;\mathcal{T})\rangle \equiv \langle\sum_{i=1}^{N}\overline{x}_i(t)\rangle \equiv \sum_{i=1}^{N}\int\prod \mathrm{d}\mathcal{T}\mathcal{P}(\mathcal{T})\overline{x}_{i-n}(t-T_n) = \\ = \sum_{n=[t/\tau_{\max}]+1}^{[t]\tau_{\max}}\mathcal{P}([t],n)\sum_{i=1}^{N}\delta_{i-n,1} = \sum_{n=[t/\tau_{\max}]+1}^{[t]\tau_{\max}}\mathcal{P}([t],n). \tag{48}$$

Here $[v]$ means the integer part of v, and we are assuming for simplicity that the duration of the initial damage is $\tau_{\mathrm{c}} = \tau_{\min} = 1$ day, hence we are using the conditions on the initial state of the system, $\{x_i(t) = \delta_{i,1}\}$ for $t \in [0, 1]$.

One has, for integer delays uniformly distributed in the interval $[\tau_{\min}, \tau_{\max}]$:

$$\langle\tau_{ij}\rangle = \int_1^{\tau_{\max}}\mathrm{d}\mathcal{T}\mathcal{P}(\mathcal{T})\tau_{ij} = \frac{(\tau_{\max}+1)}{2} \tag{49}$$

$$\sigma^2_{\tau_{ij}} = \frac{(\tau_{\max}+1)(2\tau_{\max}+1)}{6} - \frac{(\tau_{\max}+1)^2}{4}, \tag{50}$$

for the mean value and the variance of the distribution of the delays, respectively. For $n \geq 2$, assuming that the variables are independent (which is clearly an approximation for $n > N$), one can apply the central limit theorem:

$$\mathcal{P}(T_n, n) \simeq \mathcal{P}_{\mathrm{G}}(T_n, n) = \frac{1}{\sqrt{2\pi n\sigma^2_{\tau_{ij}}}}\exp\left(-\frac{(T_n - n\langle\tau_{ij}\rangle)^2}{2n\sigma^2_{\tau_{ij}}}\right). \tag{51}$$

By using this approach, we find:

$$\langle\theta(t;\mathcal{T})\rangle \simeq \begin{cases} 1 & t \in [0,1) \\ \mathcal{P}(1,1) = 1/\tau_{\max} & t \in [1,2) \\ 1/\tau_{\max} + \sum_{n=2}^{([t]\tau_{\max})} \mathcal{P}_{\rm G}([t],n) & t \in [[t],[t]+1),\ 2 \le t \le \tau_{\max} \\ \sum_{n=[t/\tau_{\max}]+1}^{([t]\tau_{\max})} \mathcal{P}_{\rm G}([t],n) & t \in [[t],[t]+1),\ t > \tau_{\max} \end{cases} \tag{52}$$

where the sums are clearly dominated by the terms corresponding to $n^*\langle\tau_{ij}\rangle \simeq [t]$, *i.e.* the same that are best approximated by the Gaussian distribution. The corresponding average density can be straightaway obtained from Eq. (10).

In the large t limit, $\langle\theta(t;\mathcal{T})\rangle$ approaches quite rapidly a nearly constant value, that in the numerically studied case of $\tau_{\max} = 10$ is found to be:

$$\lim_{t\to\infty}\langle\theta(t;\mathcal{T})\rangle \simeq \lim_{t\to\infty} \sum_{n=[[t]/\tau_{\max}]+1}^{[t]\tau_{\max}} \mathcal{P}_{\rm G}([t],n) \simeq 0.182, \tag{53}$$

which gives, again from Eq. (10):

$$\langle\rho_\infty(\mathcal{T})\rangle = \lim_{t\to\infty}\langle\rho(t;\mathcal{T})\rangle = 1 - \frac{0.182}{N}. \tag{54}$$

Appendix B Braid chain with $k \geq 2$

In this appendix, we obtain analytical estimates for the evolution in time of the average total number of impaired firms $\langle\theta(t;\mathcal{T})\rangle$ in the free model on a braid chain with with connectivity of $k = 2$ or higher, and hence for the corresponding decay rates of the density $\langle\rho(t)\rangle = 1 - \langle\theta(t;\mathcal{T})\rangle/N$ of healthy firms. By using De Morgan's law $\overline{a \wedge b} = \overline{a} \vee \overline{b}$, Eq. (12), defining the free model on the circulant matrix, turns out to be equivalent to:

$$\overline{x}_i(t) = \sum_{j=1}^{k} \overline{x}_{i-j}(t - \tau_{i,i-j}), \tag{55}$$

which, in the case of equal delays $\{\tau_{ij} = \tau_0\ \forall i,j\}$, allows the simplification:

$$\begin{aligned} \overline{x}_i(t) &= \sum_{j_1=1}^{k}\sum_{j_2=1}^{k} \overline{x}_{i-j_1-j_2}(t - 2\tau_0) = \\ &= \sum_{j_1=1}^{k}\sum_{j_2=1}^{k}\cdots\sum_{j_n=1}^{k} \overline{x}_{i-j_1-j_2-\ldots-j_n}(t - n\tau_0) = \\ &= \sum_{j=n}^{nk} \overline{x}_{i-j}(t - n\tau_0), \end{aligned} \tag{56}$$

since the different terms containing the same argument are redundant. Hence, by choosing $n = [t/\tau_0] = [t]$, one gets:

$$\theta(t) = \sum_{i=1}^{N} \overline{x}_i(t) = \sum_{j=[t]}^{[t]k} \overline{x}_{i-j}(t - [t]) = [t](k-1) + 1 \text{ for } t \in [[t],[t]+1), \tag{57}$$

where we are assuming $[t](k-1)+1 \le N$, and we used the conditions on the initial state of the system, $\{\overline{x}_{i-j}(t) = \delta_{i-j,1} \text{ for } t \in [0,\tau_{\rm c})\}$, by considering for simplicity a duration of the initial damage $\tau_{\rm c} = \tau_0$. This analysis confirms that, as soon as $k \geq 2$, the system is dissipative, and in particular the total number of impaired firms (a constant function in each time step) is linearly increasing with time, with slope $k-1$. Correspondingly, for a finite size N, the asymptotically stable solution $\{x_i \equiv 0\ \forall i\}$, and the zero limit

value of the density, are attained after the time $T_0 \simeq (N-1)/(k-1)$, in agreement with Eq. (16). One can moreover analogously show that, for $\tau_c \neq \tau_0$, the density is still linearly decreasing with time, and the asymptotic solution is the same as for $\tau_c > \tau_0$, whereas it is periodic of period τ_0 for $\tau_c < \tau_0$, as described in Section 3.4.

In order to work out the same approach for randomly distributed delays, we label $l_h = \sum_{v=1}^{h} j_v$. One finds:

$$\begin{aligned}\overline{x}_i(t) &= \sum_{j_1=1}^{k}\sum_{j_2=1}^{k}\cdots\sum_{j_n=1}^{k}\overline{x}_{i-l_n}\left(t-\sum_{h=0}^{n}\tau_{i-l_h,i-l_{h+1}}\right) = \\ &= \sum_{j=n}^{nk}\sum_{\{l_1,l_2,\ldots,l_n\}:l_n=j}\overline{x}_{i-j}\left(t-\sum_{h=0}^{n}\tau_{i-l_h,i-l_{h+1}}\right). \end{aligned} \tag{58}$$

Since the $\{\tau_{ij}\}$ are independent identically distributed random variables which take integer values (in $\tau_{\min}$ unities) in the interval $[1,\tau_{\max}]$, it follows that their sums $\mathcal{T}_n = \sum_{h=0}^{n}\tau_{i-l_h,i-l_{h+1}}$ take integer values in the interval $[n, n\tau_{\max}]$ with probability $\mathcal{P}(\mathcal{T}_n, n)$; moreover, terms $\overline{x}_{i-j}$ with the same argument are redundant. The average over the disorder can be therefore computed as:

$$\begin{aligned}\langle\overline{x}_i(t)\rangle &= \int\prod d\mathcal{T}\mathcal{P}(\mathcal{T})\overline{x}_i(t) = \\ &= \sum_{j=n}^{nk}\sum_{\mathcal{T}_n=n}^{n\tau_{\max}}\mathcal{P}(\mathcal{T}_n,n)\overline{x}_{i-j}(t-\mathcal{T}_n). \end{aligned} \tag{59}$$

Then, one can choose in particular n values in the different terms such that $t-\mathcal{T}_n$ is always in the initial interval; in detail, looking for simplicity only at t values which are integer multiple of $\tau_{\max}$, one has:

$$\begin{aligned}\langle\overline{x}_i(t)\rangle &= \left[\sum_{j=t}^{kt}\mathcal{P}_t(t,t) + \sum_{j=t-1}^{k(t-1)}\mathcal{P}_t(t,t-1) + \ldots\right. \\ &\left.\ldots + \sum_{j=t/\tau_{\max}}^{kt/\tau_{\max}}\mathcal{P}_t(t,t/\tau_{\max})\right]\overline{x}_{i-j}(0) = \\ &= \sum_{j=t/\tau_{\max}}^{t}\sum_{n=j}^{kj}\mathcal{P}_t(t,j)\delta_{i-j,1}, \end{aligned} \tag{60}$$

and therefore, up to the time $T_0(\mathcal{T})$ at which $\langle\theta(T_0(\mathcal{T});\mathcal{T})\rangle \simeq N$, one has:

$$\langle\theta(t;\mathcal{T})\rangle = \sum_{n=t/\tau_{\max}}^{t}[(k-1)n+1]\mathcal{P}_t(t,k). \tag{61}$$

Here, $\mathcal{P}_t(t,n)$ is the probability for the signal to have propagated n steps along the chain at time t, which can be approximated by a Gaussian with mean value $n\langle\tau_{ij}\rangle$ and variance $n\sigma_{i,j}^2$ (see Eq. (51)), but needs to be correctly normalized in order to get:

$$\sum_{n=t/\tau_{\max}}^{t}\mathcal{P}_t(t,n) = 1 \quad \forall t. \tag{62}$$

In detail, we take $\mathcal{P}_t(t,n) \simeq C(t)\mathcal{P}_G(t,n)$, where the normalization constant $C(t)$ approaches rapidly its large time limit $C_\infty \simeq 1/0.182$, in agreement with Eq. (53).

These results therefore confirm, from a different point of view, the analysis of Section 3.5; in particular, for the case of $n = 20$ and $\tau_{\max} = 10$, the density $\langle\rho(t;\mathcal{T})\rangle = 1 - \langle\theta(t;\mathcal{T})\rangle/N$ obtained with this approach is in very good agreement with the numerical data, as shown in [Fig. 6].

Appendix C Random graphs

Here we briefly recall the framework of generating functions from probability theory [Newman *et al.*, 2001; Dorogovtsev *et al.*, 2001]. Generating functions allow one to evaluate in a fairly straightforward manner the size of connected components in Erdős-Rényi random graphs. They are, moreover, well suited for generalization to DRGs and to probability distributions $\mathcal{P}(k)$ of the degree of a node other than Poisson.

One defines:

$$\mathcal{G}_0(y) = \sum_{k=0}^{\infty} \mathcal{P}(k) y^k, \tag{63}$$

which implies:

$$\mathcal{P}(k) = \frac{1}{k!} \frac{d^k}{dy^k} \mathcal{G}_0(y) \bigg|_{y=0}. \tag{64}$$

The generating function for the probability distribution $\mathcal{P}_1(k)$ to have k edges leaving a node, apart the one from which the signal arrived, is given by:

$$\mathcal{G}_1(y) = \sum_{k=0}^{\infty} \mathcal{P}_1(k) y^k = \frac{\sum_{k=0}^{\infty} (k+1)\mathcal{P}(k+1) y^k}{\sum_{k=0}^{\infty} k\mathcal{P}(k)} = \frac{\mathcal{G}'_0(y)}{z}, \tag{65}$$

and in the Erdős-Renyi random graph one has:

$$\mathcal{G}_0(y) = \mathcal{G}_1(y) = e^{z(y-1)}. \tag{66}$$

A key property of these functions is that, if $\mathcal{G}$ is the generating function for the probability of some property of an object, then the probability of the sum of the same property on l independent objects is generated by $\mathcal{G}^l$. Hence, if $\mathcal{H}_0(x)$ is the generating function for the distribution probability of the sizes of the connected components, *i.e.* of the nodes which can be reached from a randomly chosen one, and $\mathcal{H}_1(x)$ is the one of the clusters that can be reached from the end of one of the edges of a randomly chosen one, one has

$$\begin{aligned} \mathcal{H}_0(y) &= \sum_{l=0}^{\infty} \mathcal{P}(l) \left[\mathcal{H}_1(y)\right]^l = y\mathcal{G}_0[\mathcal{H}_1(y)], \\ \mathcal{H}_1(y) &= y \sum_{l=0}^{\infty} \mathcal{P}_1(l) \left[\mathcal{H}_1(y)\right]^l = y\mathcal{G}_1[\mathcal{H}_1(y)]. \end{aligned} \tag{67}$$

These equations can, in principle, be solved self-consistently. Most importantly for the problem at hand, one gets immediately the mean connected component size:

- below the transition

$$\langle s \rangle = \mathcal{H}'_0(1) = 1 + \mathcal{G}'_0(1)\mathcal{H}'_1(1) = 1 + \frac{\mathcal{G}'_0(1)}{1 - \mathcal{G}'_1(1)}, \tag{68}$$

which means, as expected in the Erdős-Rényi random graph, that

$$\langle s \rangle = \frac{1}{1-z}; \tag{69}$$

- above the transition, $\mathcal{H}_0(x)$ and $\mathcal{H}_1(x)$ can be defined as the generating functions for the probability distribution of the finite-size connected components, which have still a tree-like structure; correspondingly $H_0(1) = r < 1$, and one has

$$\begin{cases} s_{\rm gc} = 1 - r = 1 - \mathcal{G}_0(r) \\ r \quad = \mathcal{G}_1(r) \end{cases}, \tag{70}$$

which for Erdős-Rényi random graphs gives $r = e^{z(r-1)}$, *i.e.* Eq. (34).

References

Albert, R., & Barabási, A.-L. [2002]. Statistical mechanics of complex networks. Rev. Mod. Phys. **74**, 47–97.

Arrow, K. J., and Debreu, G. [1954]. The existence of an equilibrium for a competitive economy. Econometrica, **32**, 265–290.

Bak P., Chen, K., Scheinkman, J., & Woodford, M. [1993]. Aggregate fluctuations from independent sectoral shocks: Self-organized criticality in a model of production and inventory dynamics. Ricerche Economiche **47**, 3–30.

Bang-Jensen, J., and Gutin, G. Z. [2009]. *Digraphs: Theory, Algorithms and Applications*, 2nd ed. Springer-Verlag, 798 pp.

Barbosa, V. C., Donangelo, R., & Souza, S. R. [2003]. Directed cycles and related structures in random graphs: I - static properties. Physica A **321**, 381–397.

Barker, K., & Santos, J. R. [2009]. Measuring the efficacy of inventory with a dynamic input-output model. Int. J. Production Economics, **126**(1), 130–143, doi:10.1016/j.ijpe.2009.08.011.

Battiston, S., Delli Gatti, D., Gallegati, M., Greenwald, B., & Stiglitz, J. [2007]. Credit chains and bankruptcy propagation in production networks. J. Econ. Dyn. Control **31**, 2061–2084.

Bjerknes, J. [1969]. Atmospheric teleconnections from the equatorial Pacific. Mon. Wea. Rev. **97**, 163–172.

Bollobás, B. [1998]. *Modern Graph Theory.* Springer-Verlag, New York, 394 pp.

Broder, A., Kumar, R., Maghoul, F., Raghavan, P., Rajagopalan, S., Stata, R., Tomkins, A., & Wiener, J. [2000]. Graph structure in the Web. Computer Networks **39**, 309-320.

Carpenter, S. R., Kitchell, J. F., & Hodgson, J. R. [1985]. Cascading trophic interactions and lake productivity. Bioscience **35**, 634–639.

Chen, Z.-M., Ghil, M., Simonnet, E., & Wang, S. [2003]. Hopf bifurcation in quasi-geostrophic channel flow. SIAM J. Appl. Math. **64**(1), 343–368, doi: 10.1137/S0036139902406164.

Cho, S., Gordon, P., Moore, J., Richardson, H., Shinozuka, M., & Chang, S., [2001]. Integrating transportation networks and regional economic models to estimate the costs of a large urban earthquake. J. Regional Sci. **41**, 39–65.

Cobb, C., & Douglas, P. [1928]. A theory of production. Amer. Econ. Rev., **18** (1), 139–165.

Ding, D. W., Ding, Y. R., Li, L. N., Cai, Y. J., & Xu, W. B. [2009]. Structural and functional analysis of giant strong component of *Bacillus thuringiensis* metabolic network. Brazil. J. Microbiology **40**, 411–416.

Delli Gatti, D., Di Guilmi, C., Gaffeo, E., Giulioni, G., Gallegati M., & Palestrini, A. [2005]. A new approach to business fluctuations: heterogeneous interacting agents, scaling laws and financial fragility. J. Econ. Behavior & Organization **56**, 489-512.

Darby, M. S., & Mysak, L. A. [1993]. A Boolean delay equation model of an interdecadal Arctic climate cycle. Clim. Dyn. **8**, 241–246.

Dee, D., & Ghil, M. [1984]. Boolean difference equations, I: Formulation and dynamic behavior. SIAM J. Appl. Math. **44**, 111-126.

Donges, J. F., Zou, Y., Marwan, N. & Kurths, J. [2009]. The backbone of the climate network. Euro. Phys. Lett. **87** (4), 48007.

Dorogovtsev, S. N., Mendes, J. F. F. and Samukhin, A. N. [2001]. Giant strongly connected component of directed networks. Phys. Rev. E **64**, 025101–025105.

Drossel, B. [2008]. Random Boolean networks, in *Reviews of Nonlinear Dynamics and Complexity*, vol. 1 (H.G. Schuster, Ed.). Wiley-VHC, Weinheim, 227 pp.

Erdős, P., and Rényi, A. [1959]. On random graphs. Publ. Math. Debrecen **6**, 290–297.

Erdős, P., and Rényi, A. [1960]. On the evolution of random graphs. Magyar Tud. Akad. Mat. Kutaó Int. Közl. **5**, 17–51.

Erdős, P., and Rényi, A. [1961]. On the strength of connectedness of a random graph. Acta Math. Acad. Sci. Hungar. **12**, 261–267.

Gagneur, J., & Casari, G. [2005]. From molecular networks to qualitative cell behavior. FEBS Letters, **579**(8), Special Issue, 1867–1871.

Gardner, W. A., Napolitano, A., & Paura, L. [2006]. Cyclostationarity: Half a century of research. Signal Processing **86**(4), 639–697. doi:10.1016/j.sigpro.2005.06.016.

Ghil, M. [1994]. Cryothermodynamics: The chaotic dynamics of paleoclimate. Physica D **77**, 130–159.

Ghil, M., & Childress, S. [1987]. *Topics in Geophysical Fluid Dynamics: Atmospheric Dynamics, Dynamo Theory and Climate Dynamics.* Springer-Verlag, New York/Berlin/London/Paris/ Tokyo, 485 pp.

Ghil, M., & Mo, K.-C. [1991]. Intraseasonal oscillations in the global atmosphere. Part I: Northern Hemisphere and tropics. J. Atmos. Sci., 48, 752779.

Ghil, M., & Mullhaupt, A. P. [1985]. Boolean delay equations. II: Periodic and aperiodic solutions. J. Stat. Phys. **41**, 125-173.

Ghil, M., Mullhaupt, A. P., & Pestiaux, P. [1987]. Deep water formation and Quaternary glaciations. Clim. Dyn. **2**, 1–10.

Ghil, M., Zaliapin, I., & Coluzzi, B. [2008]. Boolean delay equations: A simple way of looking at complex systems, Physica D **237**, 2967–2986. doi:10.1016/j.physd.2008.07.006.

Ghil, M., Yiou, P., Hallegatte, S., *et al.* [2011]. Extreme events: Dynamics, statistics and prediction. Nonlin. Processes Geophys., accepted.

Gordon, P., Richardson, H., & Davis, B. [1998]. Transport-related impacts of the Northridge earthquake. J. Transp. Stat. **1**, 21-36.

Haimes, Y. Y., & Jiang, P. [2001]. Leontief-based model of risk in complex interconnected infrastructures. J. Infrastructure Systems **7**, 1–12.

Hallegatte, S. [2008]. An adaptive regional input-output model and its application to the assessment of the economic cost of Katrina. Risk Analysis **28**, 779–799.

Helbing, D., Lämmer, S., Witt, U., & Brenner, T. [2004]. Network-induced oscillatory behavior in material flow networks and irregular business cycles. Phys. Rev. E, **70**, 056118–056124.

Henriet, F. [2007]. Représentation d'une économie régionale comme un réseau : évaluation de l'impact économique d'une catastrophe naturelle. Rapport de stage d'option scientifique en Economie de l'Ecole Polythechnique, Paris.

Henriet, F., & Hallegatte, S. [2008]. Assessing the consequences of natural disasters on production networks: A disaggregate approach. Nota di lavoro 100.2008, Fondazione Enrico Mattei, http://ssm.com/abstract=1318335.

Henriet, F., Hallegatte, S., & Tabourier, L. [2010]. Firm-network characteristics and economic robustness to natural disasters. J. Econ. Dyn. Control, *sub judice.*

Hildebrandsson, H. H., & Teisserenc de Bort, L. P., 1907. *Les bases de la météorologie dynamique.*

Hoskins, B. J., and Karoly, D. J. [1981]. The steady linear response of a spherical atmosphere to thermal and orographic forcing. J. Atmos. Sci. **38**, 1179–1196.

Källén, E., Crafoord, C., & Ghil, M. [1979]. Free oscillations in a climate model with ice-sheet dynamics. J. Atmos. Sci. **36**, 2292–2303.

Karp, M. P. [1990]. The transitive closure of a random digraph. Random Structures and Algorithms **1**, 73–93.

Kauffman, S. A. [1993]. *The Origins of Order.* Oxford University Press, New York/Oxford, 709 pp.

Kaufman, M., Urbain, J., & Thomas, R. [1985]. Towards a logical analysis of the immune response. J. Theor. Biol. **114**, 527–61.

Klemm, K., and Bornholdt, S. [2005]. Stable and unstable attractors in Boolean networks. Phys. Rev. E **72**, 055101-1–055101-4.

Leontief, W. W. [1986]. *Input-Output Economics.* Oxford University Press, New York.

Leung, M., Haimes, Y. Y., & Santos, J. R. [2007]. Supply- and output-side extensions to the inoperability input-output model for interdependent infrastructures, J. Infrastructure Sys., **13**, 299–310.

Lian, C., Santos, J., & Haimes, Y. [2007]. Extreme risk analysis of interdependent economic and infrastructure sectors. Risk Analysis **27**, 1053–1064.

Łuczac, T., and Seierstad, T. G. [2009]. The critical behavior of random digraphs. Random Structures and Algorithms **35**, 271–293.

Mézard, M., Parisi, G., and Virasoro, M. A. [1988]. *Spin Glass Theory and Beyond.* World Scientific, Singapore, 464 pp.

Mullhaupt, A. P. [1984]. *Boolean Delay Equations: A Class of Semi-Discrete Dynamical Systems.* Ph. D. thesis, New York University [published also as Courant Institute of Mathematical Sciences Report CI-7-84, 193 pp.]

Neumann, A., & Weisbuch, G. [1992]. Window automata analysis of population dynamics in the immune system. Bull. Math. Biol. **54**, 21–44.

Newman, M. E. J. [2003]. The structure and function of complex networks. SIAM Reviews **45**, 167–256.

Newman, M. E. J. [2007]. Component size in networks with arbitrary degree distributions. Phys. Rev. E **74**, 045101R-045105R.

Newman, M. E. J., Strogatz, S. H., & Watts, D. J. [2001]. Random graphs with arbitrary degree distributions and their applications. Phys. Rev. E **64**, 026118–026123.

Nicolis, C. [1982]. Boolean approach to climate dynamics. Q. J. R. Meteorol. Soc. **108**, 707–715.

Öktem, H., Pearson, R., & Egiazarian, K. [2003]. An adjustable aperiodic model class of genomic interactions using continuous time Boolean networks (Boolean delay equations). Chaos **13**, 1167–1174.

Okuyama, Y. [2004]. Modeling spatial economic impacts of an earthquake: Input-output approaches. Disaster Prevention and Management **13** (4), 297–306.

Okuyama, Y., Hewings, G., & Sonis, M. [2004]. Measuring the economic impacts of disasters: Interregional input-output analysis using the sequential interindustry model. In *Modeling Spatial and Economic Impacts of Disasters*, Okuyama, Y., and S. Chang, Eds., Springer.

Pedlosky, J. [1987]. *Geophysical Fluid Dynamics* (2nd ed.). Springer-Verlag, New York/Heidelberg/Berlin, 710 pp.

Perelson, A. S., & Weisbuch, G. [1997]. Immunology for physicists. Rev. Mod. Phys. **69**, 1219–1268

Romanoff, E., & Levine, S. H. [1981]. Anticipatory and responsive sequential interindustry models. IEEE Trans. Sys., Man, and Cyber. **11**, 181-186.

Romanoff, E., & Levine, S. H. [1986]. Capacity limitations, inventory, and time-phased production in the sequential interindustry model. Papers in Regional Science, **59**, 73–91.

Romanoff, E., & Levine, S. H. [1989]. Economic impact dynamics of complex engineering project scheduling. IEEE Trans. Sys. Man Cyber., **19**, 232–240.

Rose, A., & Liao, S. Y. [2005]. Modeling regional economic resilience to disasters: A computable general equilibrium analysis of water service disruptions. J. Regional Sci. **45**, 75–112.

Saunders, A., & Ghil, M. [2001]. A Boolean delay equation model of ENSO variability. Physica D, **160**, 54–78.

Solomon, S., *et al.* [2007]. *Climate Change 2007: The Physical Science Basis. Contribution of Working Group I to the Fourth Assessment Report of the IPCC*, Cambridge University Press.

Solow, R. [1956]. A contribution to the theory of economic growth. Q. J. Economics, **70** (1), 65–94.

Souma, W., Fujiwara, Y., & Aoyama, H. [2001]. Small-world effects in wealth distribution. Arxiv preprint cond-mat/0108482 - arxiv.org.

Spyratos, V., Bourgeron P., & Ghil, M. [2007]. Development at the wildland-urban interface and the mitigation of forest-fire risk. Proc. Natl. Acad. Sci. USA **104**, 14272–14276.

Thomas, R., Ed. [1979]. *Kinetic Logic: A Boolean Approach to the Analysis of Complex Regulatory Systems*, Springer-Verlag, Berlin/Heidelberg/New York, 507 pp.

Tierney, K. [1997]. Business impacts of the Northridge earthquake. J. Contingencies Crisis Mgmt. **5**, 87–97.

Tsonis, A. A., & Swanson, K. L. [2008]. Topology and predictability of El Niño and La Niña networks. Phys. Rev. Lett. **100** (22), 228502-228506.

Walker, G. T., & Bliss, E. W. [1932]. World weather V. Mem. Roy. Meteor. Soc. **4**(36), 53–84.

Wallace, J. M., & Gutzler, D. S. [1981]. Teleconnections in the geopotential height field during the Northern Hemisphere winter. Mon. Wea. Rev. **109**, 784–812.

Watts, D. J. [1999]. *Small Worlds.* Princeton University Press, Princeton/Oxford, 262 pp.

Webb, G. R., Tierney, K. J., & Dahlhamer, J. M. [2002]. Predicting long-term business recover from disaster: A comparison of the Loma Prieta earthquake and hurricane Andrew. University of Delaware, Disaster Research Center, Preliminary Paper 328.

Weisbuch, G. [1991]. *Complex Systems Dynamics: An Introduction to Automata Networks.* Addison-Wesley, Boston, MA, 208 pp.

Weisbuch, G., & Battiston, S. [2007]. From production networks to geographical economics. J. Econ. Behavior & Organization **64**, 448–469.

Wolfram, S. [1994]. *Cellular Automata and Complexity: Collected Papers.* Addison-Wesley, Reading, Mass, 610 pp.

Wright, D. G., Stocker, T. F., and Mysak, L. A. [1990]. A note on Quaternary climate modelling using Boolean delay equations. Clim. Dyn. **4**, 263–267.

Zaliapin, I., Keilis-Borok, V., & Ghil, M. [2003a]. A Boolean delay equation model of colliding cascades. Part I: Multiple seismic regimes. J. Stat. Phys. **111**, 815-837.

Zaliapin, I., Keilis-Borok, V., & Ghil, M. [2003b]. A Boolean delay equation model of colliding cascades. Part II: Prediction of critical transitions. J. Stat. Phys. **111**, 839-861.

Zaliapin, I., Foufoula-Georgiou, E., & Ghil, M. [2010]. Transport on river networks: a dynamical approach. J. Geophys. Res.–Earth Surface **115**, F00A15, doi:10.1029/2009JF001281.

Zhang, R., de S. Cavalcante, H. L. D., Gao, Z., Gauthier, D. J., Socolar, J. E. S., Adams, M. M., & Lathrop, D. P. [2009]. Boolean chaos. Phys. Rev. E **80**, 045202(R)-045206(R).